

Impacts of surface chemistry and adsorbed ions on dynamics of water around detonation nanodiamond in aqueous salt solutions

Farshad Saberi-Movahed* and Donald W Brenner

Department of Materials Science and Engineering, North Carolina State University, Raleigh, NC, USA.

(*Corresponding author: fsaberi@ncsu.edu)

ABSTRACT

Water near detonation nanodiamonds (DNDs) forms a Hydrogen Bond (HB) network, whose strength influences DNDs' fluorescence intensity and colloidal stability in aqueous suspensions. However, effects of dissolved ions and DND's surface chemistry on dynamics of water that manifest in rupture and formation of HBs still remain to be elucidated. Thus, we carried out molecular dynamics simulations to investigate the aforementioned effects in the aqueous salt (any of KCl, NaCl, CaCl₂, or MgCl₂) solution of DND functionalized with any of -H, -NH₂, -COOH, or -OH groups. We observed the specific cation effects on both translational and reorientational dynamics of water around the negatively charged DND-COOH. In the whole hydration shell of this DND, we obtained $K^+ < Na^+ < Ca^{2+} < Mg^{2+}$ ordering for the impact of the cation on reducing the translational diffusion coefficient of water. In the immediate vicinity of the charged DND-COOH, the slowdown impacts of cations on the reorientational dynamics of dipole and OH vectors of water were according to $Na^+ < K^+ < Ca^{2+} < Mg^{2+}$ and $Na^+ < Ca^{2+} < K^+ < Mg^{2+}$ ordering, respectively. Furthermore, regardless of the type of dissolved ions, positively charged DND-NH₂ and negatively charged DND-COOH induced, respectively, the slowest dipole and OH reorientational dynamics in the first hydration layer of DND. Our results led us to conclude that charged groups on the surface of DNDs on the one hand and the adsorbed counterions on the other hand cooperatively slow down the reorientational dynamics of water in multiple directions.

Keywords: Nanodiamond; Functional Group; Ion; Aqueous Solution; Self-diffusion; Reorientational Dynamics; Wobbling-in-cone Motion; Molecular Dynamics Simulation.

1 Introduction

Many of exceptional properties of water, such as the unusual density of liquid water at 4 °C and relatively high surface tension, have been attributed to its hydrogen bond (HB) network¹. This network has a dynamic nature, which results from the breaking and making of HB bonds in the network due to thermal excitations. These network reconstructions are not possible without rotations and translations of the network's constituent water molecules.^{2,3} Therefore, both translational and rotational dynamics of water have been the subject of numerous studies of both experimental and theoretical nature.⁴⁻¹² In particular, specific attentions have been paid to the dynamics of the interfacial water around solutes.¹³⁻¹⁶

The motivation behind studying the dynamics of the interfacial water arises from understanding the mutual effects of solutes and water on each other. On the one hand, the functioning of certain molecules such as proteins depends on the HB network of water and its fluctuations and dynamic rearrangements around them.¹⁷⁻²³ For instance, the successful catalytic activity of enzymes requires that the corresponding proteins undergo conformational transitions as smoothly as possible. It has been suggested that the dynamic rearrangements of the interfacial water facilitate these conformational transitions.²⁴ On the other hand, some solutes such as ions can substantially modify the arrangement of their immediate surrounding water. This phenomenon

can have different manifestations in a multitude of macroscopic properties of electrolyte solutions. These effects of ions, which ultimately depend on their size and electric charge, have been referred to as “specific ion effects”.

The “specific ion effects”, was first discovered by Hofmeister in the study of protein solubility in salt solutions.²⁵ Initially, Hofmeister ordered constituent ions of salts into the so-called Hofmeister series according to their effects on the solubility and conformational stability of proteins in electrolyte solutions.²⁶ Over time, the series has been expanded to include more salts and also to explain wider range of ionic solution properties such as diffusion coefficient and viscosity.^{27,28}

Ions in the Hofmeister series have been further classified into kosmotropes (“structure-makers”) or chaotropes (“structure-breakers”).²⁹ The former, which include small ions with high surface charge densities such as Ca^{2+} or Mg^{2+} , induce highly ordered arrangements in their tightly bound hydration shells. However, the latter, which have larger size and smaller charge densities such as K^+ or Cl^- ions, are characterized by disorganized water structure and weakened HB in their surroundings.^{30,31} Recent studies have shown that these structural perturbations are limited to the first hydration shell of most ions, except in certain conditions. More specifically, if both cation and anion of a salt possess high surface charge densities, they can cooperatively slow down the reorientational dynamics of water well beyond their first hydration shells.^{32–34} This thereby can lead to locking in the HB network of water in multiple directions.³⁵

To the best of our knowledge, the dynamics of hydration shells of Detonation Nanodiamond (DND) in electrolyte solutions have not been studied yet, despite their promising biomedical applications such as anti-cancer drug delivery^{36–39}, treatments for neurodegenerative diseases⁴⁰, and bioimaging⁴¹. In these applications, DNDs are inevitably in contact with water, certain ions, and some other residues^{42–45}. In particular, it has been shown that the HB network of water plays an important role in fluorescence properties of DNDs.⁴⁶

We therefore aimed at investigating the dynamics of water in the hydration shells of DNDs in aqueous solution of inorganic salts. The center of our attention is placed on the effects of the surface chemistry of DNDs, on the one hand, and the solvated salts, on the other hand, on the translational and orientational dynamics of the interfacial water. Particularly, our main objective is to find out the underlying mechanism behind the reorientation of water in the hydration shells, which has paramount implications for HB network reconstructions.

In order to study the translational dynamics of the interfacial water, we have calculated its self-diffusion coefficient using the well-known Einstein relation⁴⁷. Then, we have developed a multiple regression model, which describes the relationship between the self-diffusion coefficient of the interfacial water, on the one hand, and the DNDs’ surface chemistry and solvated salts on the other hand.

To study the rotational dynamics of the interfacial water, we have defined reorientational correlation functions (RCF) to track the time evolution of water’s dipole moment and OH bond reorientations. In a sense, these functions, which have been extensively used in the literature⁴⁸, demonstrate how quickly water loses the memory of its original orientations³. As pointed out in many studies^{4,19,32,49–54}, there are multiple timescales in the decay behavior of RCFs. We have used the extended wobbling-in-a-cone (EWIC) model in order to interpret these multiscale reorientational relaxations.^{10,52,55,56} This has eventually led us to propose a cooperative mechanism for the rotational dynamics of water in hydration shells of charged DNDs surrounded by counterions. We have presented the details of this mechanism in the remainder of this paper.

We have utilized the classical Molecular Dynamics (MD) simulation^{57,58} to carry out the studies explained above. It serves as a great tool to realize our goals for two reasons. First, we can readily use the resulting atomic trajectories to calculate the Mean Squared Displacements (MSD) of water oxygen atoms, which eventually gives us the self-diffusion coefficient of the interfacial water using the Einstein relation. Second, it has been shown that MD simulations have this benefit over most experimental techniques that can capture all three timescales of the reorientational relaxations of the interfacial water.^{3,10,52} In addition, the explicit representation of water in the fully atomistic MD simulation enables us to readily identify water orientations along its dipole moment and OH bonds.

The rest of the present paper is organized as follows. We have described the MD simulation setup as well as the utilized computational tools in Section 2. The self-diffusion coefficient of the interfacial water as well as the corresponding multiple regression model are presented in Section 3. Then, we have demonstrated the RCF plots in Section 4 and have discussed the reorientational behavior of water in hydration shells of DNDs and ions. The cooperative mechanism for water's rotational dynamics nearby charged DNDs is also discussed. Finally, we have summarized our important findings in Section 5.

2 Methodology

2.1 MD simulation setup

Each atomistic system in our MD simulations consists of a single cuboctahedral DND of 4.4 nm in diameter with a distinct surface chemistry, solvated in 0.1M aqueous solution of any of KCl, NaCl, CaCl₂, or MgCl₂ salts. The charge density of ions making up these salts varies in the order Cl⁻ < K⁺ < Na⁺ < Ca²⁺ < Mg²⁺. Four types of surface functionalizations for DNDs are considered, namely, fully hydrogenated (DND-H), hydroxylated (DND-OH), carboxylated (DND-COOH), and aminated (DND-NH₂). The last three types of DNDs also have some amounts of hydrogen on their surfaces. Furthermore, DND-OH exists as an electrically neutral particle in the present work, while all other DNDs have both neutral and charged variants. The charged versions of DND-COOH and DND-NH₂ are created by adding -COO⁻ and -NH₃⁺ to their respective facets, while the charged DND-H is obtained via a charge equilibration method⁵⁹. The detailed, step-by-step procedure that we took to run the MD simulations is described elsewhere⁶⁰.

2.2 Computational Tools

In this section, we introduce some computational tools that we have developed as adds-on to MDAnalysis^{61,62} package. We have used them to post-process the atomic trajectories for characterizing dynamics of water in hydration layers around solutes. The tools are implemented in python codes, which incorporate the Message Passing Interface (MPI) for parallel computing to distribute heavy computations on massive atomic data across high-performance computing clusters.

2.2.1 Self-diffusion Coefficient

The self-diffusion coefficient is often employed in MD simulations to characterize the translational motions of atomic systems. Furthermore, it is viable to experimentally measure the self-diffusion coefficient using various Nuclear Magnetic Resonance (NMR) techniques^{63,64}, hence it provides a validation tool for MD results. In the present study, we are particularly interested in quantifying the effects of DND's surface functional groups and charge density, on the one hand, and dissolved ions, on the other hand, on the translational mobility of water molecules.

The self-diffusion coefficient D of atoms in a 3D system can be obtained from the Einstein relation⁴⁷ as

$$D = \lim_{t \rightarrow \infty} \frac{\langle [\vec{r}(t) - \vec{r}(t_0)]^2 \rangle}{6t} \quad \text{Eq. 1}$$

where the numerator is the MSD, $\vec{r}(t)$ is the coordinate vector of the atom at time t , t_0 denotes different starting times, and $\langle \dots \rangle$ is the ensemble average. The Einstein relation tells us that if the MSD vs. time curve turns out to be linear, then its slope divided by 6 gives the self-diffusion coefficient.

2.2.2 Reorientational Correlation Function

To obtain a more complete picture of effects of ions and DNDs on the dynamics of water in DNDs' hydration layers, we also need to study the rotational dynamics of water. For this purpose, we use the Reorientational Correlation Function (RCF)⁴⁸ defined as

$$C_2^u(t) = \frac{\langle P_2[\vec{u}(t) \cdot \vec{u}(t_0)] \rangle}{\langle P_2[\vec{u}(t_0) \cdot \vec{u}(t_0)] \rangle} \quad \text{Eq. 2}$$

where P_2 is the Legendre polynomial of order 2, $\vec{u}(t)$ is the unit vector along the orientation of interest \vec{u} , t_0 represents different starting points in time, and $\langle \dots \rangle$ denotes the ensemble average. In this study, we have investigated RCFs for water's orientations along its dipole moment ($\vec{\mu}$) and OH bonds (see Figure 1(a)). Hereafter, we denote their corresponding correlation functions and related parameters with superscripts *dip* and *oh* (e.g., $C_2^{dip}(t)$ and $C_2^{oh}(t)$), respectively. It is worth noting that $C_2^u(t)$ can be measured via various experimental techniques, of which an in-depth review can be found elsewhere³.

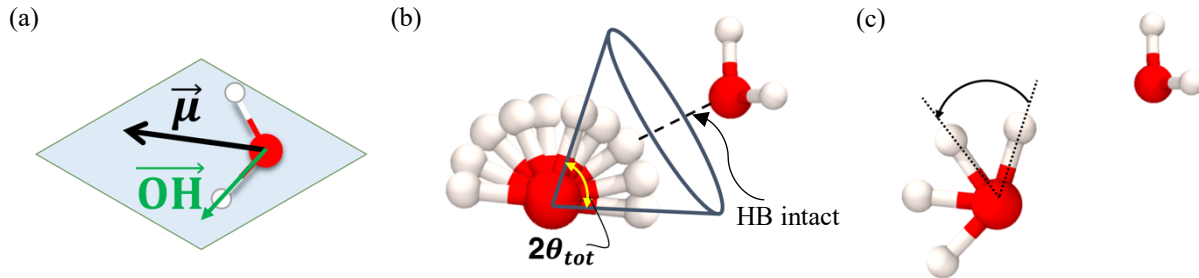


Figure 1. (a) Two different orientations of water, that is, dipole moment ($\vec{\mu}$) and $\overline{\text{OH}}$ bond, (b) the hypothetical cone in which $\overline{\text{OH}}$ bond of water carries out inertial and wobbling diffusive motions, both of which result from restricted rotation due to the intact HB with the nearby water, (c) unrestricted rotation of the water molecule that has broken the HB with its neighbor.

In spite of the simple mathematical expression for $C_2^u(t)$, its decay behavior involves complex mechanisms that contribute to the reorientational dynamics of water. Indeed, numerous experimental and theoretical studies have shown that water's reorientational relaxation in confined environments takes place at three different timescales, independent of each other.⁶ To provide a concrete interpretation for the multiscale decay of RCFs, we have adopted the extended wobbling-in-a-cone (EWIC) model^{10,52,55}. The EWIC model fits a tri-exponential function to $C_2^u(t)$, which is written as

$$C_2^u(t) = \underbrace{\left[(T^u)^2 + (1 - (T^u)^2) \exp\left(-\frac{t}{\tau_{in}^u}\right) \right]}_{\text{Inertial motion in a cone with semi-angle } \theta_{in}^u} \times \underbrace{\left[(S^u)^2 + (1 - (S^u)^2) \exp\left(-\frac{t}{\tau_c^u}\right) \right]}_{\text{Wobbling motion in a cone with semi-angle } \theta_c^u} \times \underbrace{\exp\left(-\frac{t}{\tau_m^u}\right)}_{\text{Final unrestricted diffusive motion}} \quad \text{Eq. 3}$$

According to the EWIC model, water molecules first undergo an inertial-liberational motion in a cone with the semi-angle of θ_{in}^u , followed by wobbling motions in a cone with a larger semi-angle θ_c^u than θ_{in}^u (see Figure 1(b)). Finally, the rotational diffusion of water without angular restrictions leads to its complete orientational randomization (see Figure 1(c)). In a sense, these three rotational modes of water have been reflected in the functional form of the EWIC model in Eq. 3. That is, the inertial reorientation decays with the relaxation time τ_{in}^u to a plateau, which is further decayed by the wobbling diffusive motion in the cone to a second plateau with the relaxation time constant of τ_c^u . The second plateau is then further decayed by the final rotational diffusion process with the relaxation time τ_m^u . While the relaxation of the liberational reorientation and the wobbling diffusion occur, respectively, on sub-ps and ~ 1 -ps timescales, the final rotational diffusion process has the relaxation timescales of 10s-100s ps.

Tan *et al.* have related the angularly restricted (i.e., liberational and wobbling) and unrestricted (rotational diffusion) modes of water reorientations to the dynamics of water's HB network.⁵² While the former reflects the local fluctuations in the HB network without breaking the HBs, the latter leads to the breaking and making of HBs and hence is thought of as a global process. According to the EWIC model, we can quantify these local and global processes by using, respectively, the wobbling diffusion coefficient D_c^u and the rotational diffusion coefficient D_m^u , which are defined as:

$$D_c^u = \frac{(x_c^u)^2(1+x_c^u)^2\{\ln[(1+x_c^u)/2] + (1-x_c^u)/2\}}{\tau_c^u(1-(S^u)^2)[2(x_c^u-1)]} + \frac{(1-x_c^u)(6+8x_c^u-(x_c^u)^2-12(x_c^u)^3-7(x_c^u)^4)}{24\tau_c^u(1-(S^u)^2)} \quad \text{Eq. 4}$$

$$(S^u)^2 = \left[\frac{1}{2} (\cos \theta_c^u)(1 + \cos \theta_c^u) \right]^2 \quad \text{Eq. 5}$$

$$D_m^u = \frac{1}{6\tau_m^u} \quad \text{Eq. 6}$$

where $x_c^u = \cos \theta_c^u$. We can replace $(S^u)^2$ by $(T^u)^2(S^u)^2$ in Eq. 5 to obtain the total cone angle θ_{tot}^u , which denotes angles sampled by both inertial and wobbling diffusive motions (see Figure 1(b)). Furthermore, we calculate the orientational correlation time⁶⁵, τ_{corr}^u , as the time integration of $C_2^u(t)$

$$\tau_{corr}^u = \int_0^\infty C_2^u(t) dt \quad \text{Eq. 7}$$

For the completeness of the discussion, we need to briefly mention a different competing model, called the Extended Jump Model (EJM)^{66,67}, which has recently attracted some attentions^{19,68}. This model involves two unequally weighted contributions to the reorientation of water in its local environment: 1) dominant contributions from the exchange of HB acceptors, which leads to sudden large amplitude jumps of water's OH bonds, 2) angular diffusive rotations of intact HBs in between the jumps. Although the first mode of EJM is absent in the EWIC model, the second contribution to water reorientations resembles to the diffusive wobbling motion of water's orientations in the hypothetical cone. However, EJM only focuses on the local changes in

the orientation of water and does not explain the final rotational diffusion process, which leads to the global reconstructions in the HB network³. Thus, we decided to adopt the EWIC in our study.

To calculate RCFs, we have sampled conformations during MD simulations every 100 steps from the last 200 ps of the NVT production run. It means that the sampling time window is 0.1 ps given that every MD step is 1 fs. The rationale behind this choice is twofold. First, it helps capture the fast, sub-picosecond mode of the reorientational dynamics to some acceptable extent. Secondly, if we had chosen smaller frequencies to save atomic trajectories, the computational task would have been prohibitively difficult.

3 Results and Discussions

3.1 Translational dynamics

We study the translational motion of water around DNDs by measuring water’s self-diffusion coefficient D . The Einstein relation (see Eq. 1) gives D as the slope of the MSD vs. time, provided that they are linearly related. We calculated MSDs of water’s oxygen atom in the whole hydration shell of various DNDs solvated in different salt solutions. The whole hydration shell is defined as a 1 nm thick spherical shell around the DND and centered at its centroid, beyond which water has a bulk-like behavior. Roughly speaking, it is an aggregation of the first to the third hydration layers of the DND, which we had identified in our previous study⁶⁰. Our initial goal was to calculate the self-diffusion coefficient of water in each of the first, the second, and the third hydration layers of DNDs. However, the relatively small number of water molecules in those layers makes the MSD of water suffer from a lack of sufficient statistical sampling. Thus, we instead decided to calculate the self-diffusion coefficient of water in the whole hydration layer.

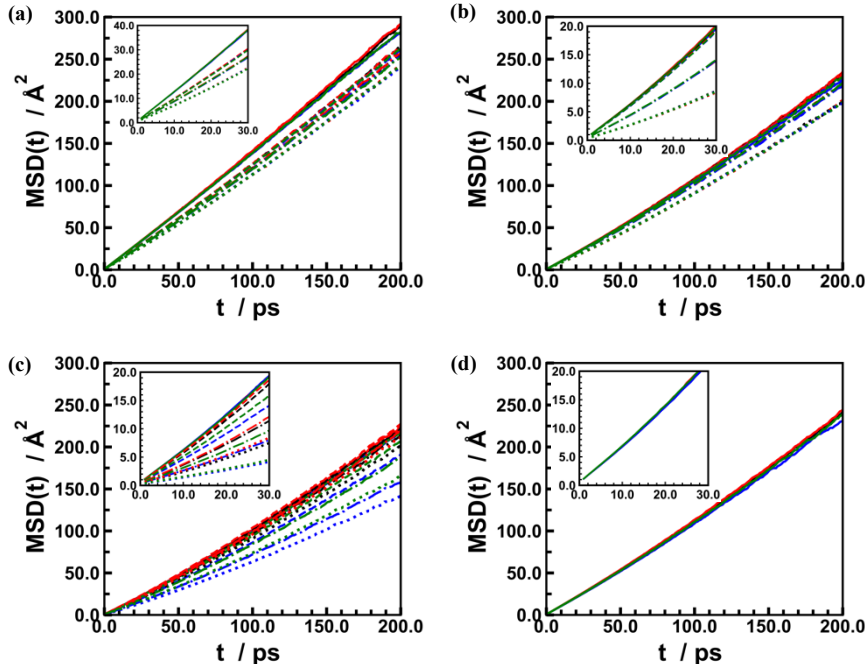


Figure 2. MSDs of water in the whole hydration layer of different DNDs with various surface charges that are solvated in four different salt solutions: KCl (red line), NaCl (black line), CaCl_2 (green line), MgCl_2 (blue line). (a) DND-H, (b) DND-NH₂, (c) DND-COOH, (d) DND-OH. Solid, dashed, dash-dotted, and dotted lines correspond to 0, 28, 56, and 84 absolute charges on DNDs, respectively. DND-H and DND-NH₂ assume any of these charges with the positive sign, so does DND-COOH but with the negative sign. But DND-OH only exists as a neutral particle in our study.

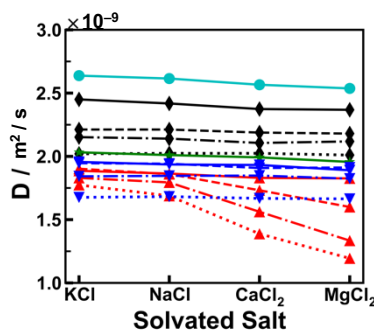


Figure 3. Self-diffusion coefficient of water in the whole hydration layer of different DNDs with various surface charges (differentiated by different line styles). Black, blue, red, and green lines represent DND–H, DND–NH₂, DND–COOH, and DND–OH particles, respectively. Line styles are the same as those in Figure 2. The cyan line shows the self-diffusion coefficient of water in the bulk region of the neutral DND–H solvated in four different salt solutions.

We have shown the calculated MSDs in Figure 2, in which we observe a linear relationship between MSD and time. Thus, we can readily obtain the self-diffusion coefficients of the DNDs’ hydrating water as the slope of MSD plots. In Figure 3, we have compared the effects of different salts on the resulting D values corresponding to various DNDs. We have also shown the self-diffusion coefficients of water in the bulk region of the neutral DND–H solutions far away from the influence of DNDs’ surfaces. The numerical values of D as well as the standard error of the linear regression fit are presented in the Supplementary Information (SI) (Table S.1 to Table S.5). We observe couple of interesting trends in Figure 3 that are discussed below.

First, water diffuses the fastest around the uncharged DND–H compared with other uncharged DNDs and it has the closest self-diffusion coefficient to that of the bulk water. It implies that water surrounding DND–H with zero net charge has a bulk-like behavior in terms of the translational motion. We ascribe this behavior to the hydrophobic nature of the DND–H surface, which does not form any HBs with the interfacial water, as opposed to other DNDs in this study. In contrast, surfaces of DND–OH, DND–NH₂, and DND–COOH particles are covered with polar groups, which can form HBs with the interfacial water molecules. Thus, they can slow down the motion of the nearby water molecules.

Second, with some few exceptions, the self-diffusion coefficients decrease with increases in the net charge of DNDs. The exceptions are DND–NH₂ with +28 net charge solvated in any of salt solutions and DND–COOH with –28 net charge that is solvated in either KCl or NaCl solutions. As opposed to the uncharged DND–NH₂, DND–NH₂ with +28 net charge has twenty-eight NH₃⁺ groups on its surfaces. However, it seems they are not sufficient to enhance the formation of strong HBs with the interfacial water.

Third, the negatively charged DND–COOH has a distinct effect on the retardation of water compared with the positively charged DND–H and DND–NH₂. In particular, different positive counterions (i.e., Na⁺, K⁺, Ca²⁺, Mg²⁺) present in the vicinity of the charged DND–COOHs have contrasting impacts on the mobility of water molecules in the aforementioned hydration shells. Indeed, we can rank them based on their association with the relative slowdown of the water mobility in the whole hydration shell of the charged DND–COOH as

$$\text{Mg}^{2+} (0.72/4.3) > \text{Ca}^{2+} (1.0/2.24) > \text{Na}^{+} (1.02/1.06) > \text{K}^{+} (1.38/0.59)$$

The numbers inside the parentheses denote ionic radius in Å and the relative charge density of cations, respectively.⁶ We also observe the same trend in the self-diffusion coefficients of the bulk water in the corresponding chloride-cation salt solutions.

The aforementioned ranking follows the Hofmeister series^{9,31}, which suggests that ions with larger charge densities are associated with more pronounced effect on the retardation of water molecules. In particular, if we only compare isovalent ions with each other, water surrounded by the smaller ion species experiences more slowdown in its mobility. We can attribute this effect to the stronger binding energies between smaller cations, which have higher charge densities, and water molecules in the cations' first hydration shell. In Fact, calculations of the entropy of hydration of alkaline metal cations and also halide anions have revealed that K^+ and Cl^- ions weakly bind water molecules, while Na^+ strongly bind water molecules compared with water-water interactions in the pure water.^{69,70} Hence, water molecules are more mobile in the surroundings of K^+ cations, compared with those around Na^+ . Interestingly, it matches quite well with our findings in Figure 3, where we found that the self-diffusion of water around the negatively charged DND–COOH is lower in the presence of adsorbed Na^+ cations than that of K^+ .

To investigate the statistical significance of differences we observed in Figure 3, we have developed the following multiple regression model for self-diffusion coefficient of water molecules in the whole hydration shell of DNDs.

$$D = \beta_0 + \beta_1 \text{charge} + \beta_2 \text{DND} + \beta_3 \text{DND:charge} + \beta_4 \text{salt:DND:charge} \quad \text{Eq. 8}$$

where β_i is the regression coefficient, *DND* corresponds to one of DND particles (DND–H, DND–COOH, DND–NH₂), *charge* is the number of charges on the DND, and *salt* is the solvated salt in water (NaCl, KCl, MgCl₂, CaCl₂). β_3 and β_4 are coefficients of the so-called interaction terms between, respectively, (*DND*, *charge*) and (*salt*, *DND*, *charge*). The regression model can help us assess the statistically significance of the effects of DND's surface charges and also the type of the salt on the mobility of DND's interfacial water. Particularly, interaction terms facilitate to investigate whether *charge* or *salt* modifies the effect of DND's surface moieties on the interfacial water's self-diffusion coefficient.

Table 1. Coefficients of the regression model in Eq. 8. We have assigned DND–COOH and KCl as reference levels to categorical variables *DND* and *salt*, respectively. Values of β_i , Standard Error, and confidence interval are expressed in $10^{-9} \text{ m}^2 \cdot \text{sec}^{-1}$.

Variable	β_i	Standard Error	p-value	95% confidence interval
Intercept (β_0)	1.8660	0.0082	0.0	(1.8500, 1.8800)
<i>charge</i>	-0.0008	0.0002	0.0	(-0.0013, -0.0004)
<i>DND</i> = DND–NH ₂	0.1040	0.0116	0.0	(0.0811, 0.1270)
<i>DND</i> = DND–H	0.5037	0.0116	0.0	(0.4810, 0.5270)
<i>DND</i> = DND–NH ₂ : <i>charge</i>	0.0038	0.0003	0.0	(0.0031, 0.0044)
<i>DND</i> = DND–H : <i>charge</i>	0.0050	0.0003	0.0	(0.0044, 0.0056)
<i>salt</i> = NaCl : <i>DND</i> = DND–COOH : <i>charge</i>	-0.0009	0.0003	0.0	(-0.0015, -0.0004)
<i>salt</i> = CaCl ₂ : <i>DND</i> = DND–COOH : <i>charge</i>	-0.0048	0.0003	0.0	(-0.0053, -0.0042)
<i>salt</i> = MgCl ₂ : <i>DND</i> = DND–COOH : <i>charge</i>	-0.0077	0.0003	0.0	(-0.0083, -0.0072)
<i>salt</i> = NaCl : <i>DND</i> = DND–NH ₂ : <i>charge</i>	-0.0001	0.0003	0.833	(-0.0006, 0.0005)
<i>salt</i> = CaCl ₂ : <i>DND</i> = DND–NH ₂ : <i>charge</i>	0.0001	0.0003	0.631	(-0.0004, 0.0007)
<i>salt</i> = MgCl ₂ : <i>DND</i> = DND–NH ₂ : <i>charge</i>	0.0003	0.0003	0.309	(-0.0003, 0.0008)
<i>salt</i> = NaCl : <i>DND</i> = DND–H : <i>charge</i>	0.0000	0.0003	0.908	(-0.0005, 0.0006)
<i>salt</i> = CaCl ₂ : <i>DND</i> = DND–H : <i>charge</i>	0.0003	0.0003	0.319	(-0.0003, 0.0008)
<i>salt</i> = MgCl ₂ : <i>DND</i> = DND–H : <i>charge</i>	0.0003	0.0003	0.213	(-0.0002, 0.0009)

The dataset, which has been used to fit the regression model, contains 240 observations, wherein each combination of *DND*, *charge*, and *salt* has self-diffusion coefficients calculated from five independent MD simulations. The fitted model has a high adjusted- R^2 of 0.972 and its coefficients are listed in Table 1.. Since *DND* and *salt* variables are categorical, their corresponding values of β_i are given for each specific level of the categorical variable. In this regard, we have assigned, respectively, DND-COOH and KCl as the reference level to the former and latter. Thus, β_0 corresponds to the self-diffusion coefficient of water in the whole hydration shell of DND-COOH in KCl solution, adjusted for the DND's charges.

With the significance level of 5%, we discard all regression coefficients in Table 1., whose p-values are larger than 0.05. Thus, our model shows that the effect of the solvated salt on the mobility of the DND's interfacial water is statistically significant only for negatively charged DND-COOHs. In contrast, the effect of the amount of DND's surface charges on its interfacial water mobility is not only statistically significant for all types of DNDs, but also this effect gets modified depending on the type of DND. The latter statement is supported by the p-values of the *DND:charge* interaction term in Table 1.. These two conclusions match with the trends we previously observed in Figure 3. Based on the explanations above, the final form of the multiple regression model for the self-diffusion coefficient becomes:

$$\begin{aligned}
 D = & 1.866 - 0.0008 \times \text{charge} \\
 & + 0.1040 \times (\text{DND} - \text{NH}_2) + 0.5037 \times (\text{DND} - \text{H}) \\
 & + 0.0038 \times (\text{DND} - \text{NH}_2): \text{charge} + 0.0050 \times (\text{DND} - \text{H}): \text{charge} \\
 & - 0.0009 \times \text{NaCl}: (\text{DND} - \text{COOH}): \text{charge} \\
 & - 0.0048 \times \text{CaCl}_2: (\text{DND} - \text{COOH}): \text{charge} \\
 & - 0.0077 \times \text{MgCl}_2: (\text{DND} - \text{COOH}): \text{charge}
 \end{aligned}
 \tag{Eq. 9}$$

3.2 Rotational dynamics

We now turn our attention to the rotational dynamics of water molecules in the vicinity of DNDs. For this purpose, we have calculated the RCF for dipole and OH vectors of DNDs' interfacial water.

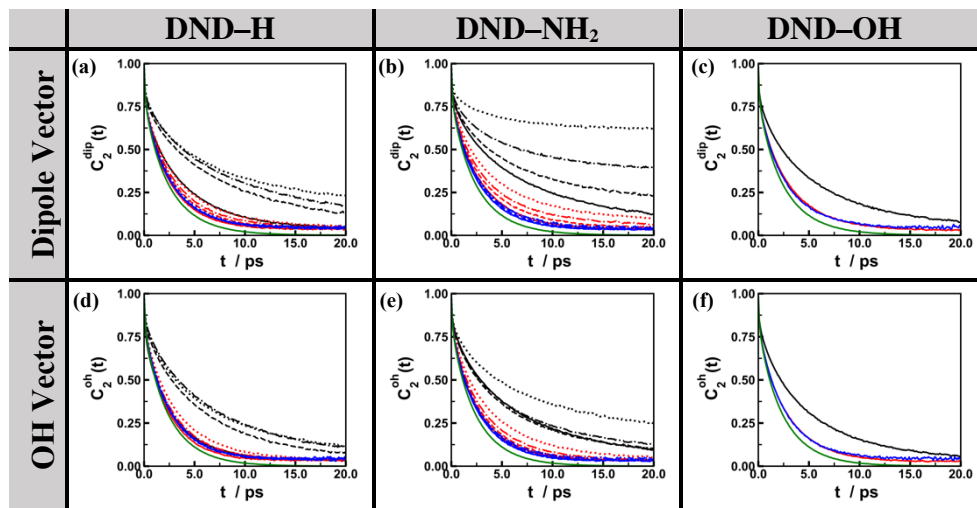


Figure 4. RCFs of two water's orientations, dipole and OH vectors, in the first (black line), second (red line), and third (blue line) hydration layers of different DNDs with various surface charges (differentiated by different line styles) that are solvated in NaCl solution. Line styles are the same as those in Figure 2. RCFs of these DNDs in other three salt solutions are almost identical to ones shown here.

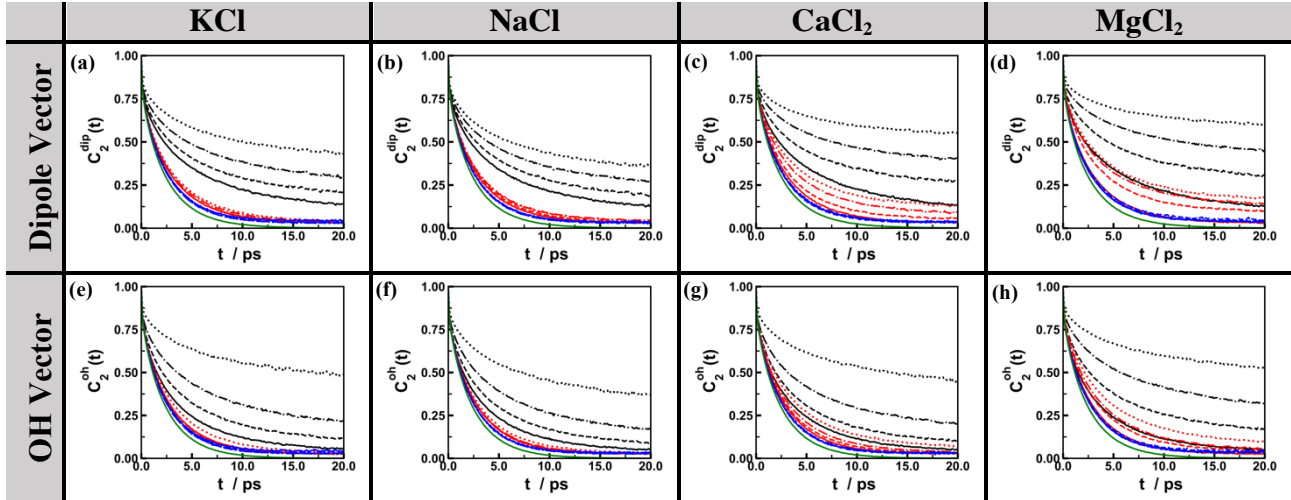


Figure 5. Same as Figure 4, but for DND–COOH in four different salt solutions: KCl, NaCl, CaCl₂, MgCl₂.

We have shown the time evolution of RCFs in Figure 4 for DND–H, DND–NH₂, and DND–OH, which are solvated in the NaCl salt solution. Since results for other three salt solutions resemble to those of NaCl salt solution, they have not been included in Figure 4. In contrast, there seems to be an association between the type of the cation in the solution and the decay rate of RCFs for DND–COOHs. Thus, we have demonstrated RCFs for water around DND–COOH in Figure 5, which have been distinguished by the type of the salt in the solution. All plots in these two figures include results for all three hydration layers. We had previously identified these hydration layers elsewhere⁶⁰.

We observe three distinct behaviors in the reorientational dynamics of water shown in Figure 4 and Figure 5:

- 1) Water in the first and second hydration layers of DNDs, except for DND–OH, exhibits anisotropy in the decay rate of its dipole and OH vectors' reorientation. The anisotropic decay appears to be more prominent, as DNDs become more positively or negatively charged, particularly in the case of DND–COOH and DND–NH₂ systems.
- 2) We observe an apparent interaction between the influence of surface charges of DND–COOH and the type of the solvated salt on the RCF decay of both dipole and OH orientations. This trend is similar to what we observed for the translational mobility of DNDs' interfacial water in the previous section. As we pointed out before, the negatively charged DND–COOH attracts cations to its first hydration layer, while positively charged DND–H and DND–NH₂ accumulate Cl[−] counterions at their interface with water. Since alkali metal and alkaline earth cations have different binding strength with water, they have differing impacts on its various orientational degrees of freedom.
- 3) All RCFs appear to decay at multiple distinct time scales. They undergo a fast decay, followed by slower relaxations. In particular, when DNDs acquire more surface charges, the slower relaxation visually becomes more obvious.

We use the EWIC model, introduced in Section 2, to quantify the aforementioned different relaxation time scales of RCFs. Furthermore, this model enables us to elucidate the impact of DND's surface chemistries and solution environments on the reorientational dynamics of the interfacial water.

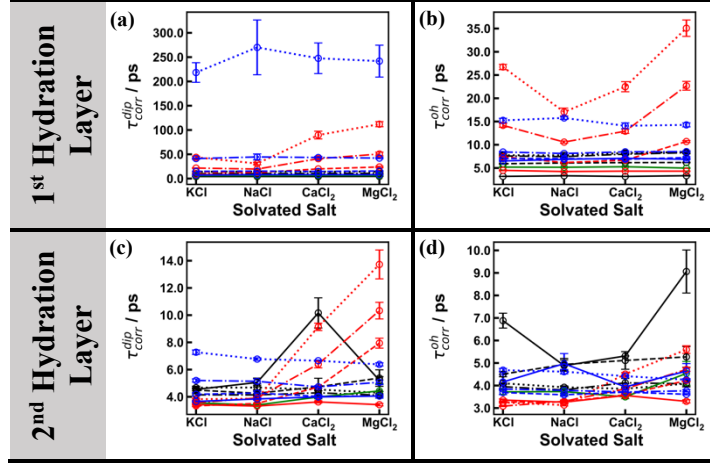
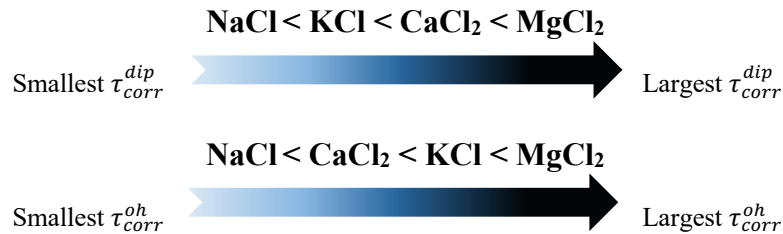


Figure 6. Correlation time of RCFs for dipole and OH orientations of water, denoted as τ_{corr}^{dip} and τ_{corr}^{oh} , in the first and second hydration layers of DNDs. Lines' styles and colors are the same as those in Figure 3.

We have listed relaxation time constants along with other parameters associated with the EWIC model in the SI (Table S.6 through Table S.21). Following statements hold true for both dipole and OH vectors of water. The scale of relaxation time constants, τ_{in} , τ_c , and τ_m in these tables confirms the existence of three regimes in the orientational relaxation of water that we discussed in Section 2. More specifically, τ_{in} with sub-picosecond values corresponds to very fast inertial-liberational orientational motion, while τ_c exhibits values on a larger scale of ~ 1 -5 picoseconds. The latter characterizes the constraint rotational diffusion in a cone. In addition, we can observe values as small as ~ 10 picoseconds and as large as ~ 200 -400 picoseconds for τ_m , which characterize the final much slower reorientational relaxations. The largest values of τ_m correspond to reorientational relaxation of water's dipole moment in the first hydration layer of DND-NH₂ with +84 absolute charges. It points to the existence of substantial constraints on the water's dipole reorientation in the aforementioned region.

In Figure 6, we have demonstrated the correlation time of RCFs for dipole and OH vectors of water in the first and second hydration layers around DNDs. We have discussed below some interesting patterns that we have found in this figure.

- 1) The interaction between the absolute net charges of DND-COOHs and the type of solvated salt that we observed in Figure 5 is also reflected in the correlation time of RCF (i.e., τ_{corr}) for dipole (see Figure 6((a), (c)) and OH (see Figure 6((b), (d))) vectors. In fact, we can sort the salts in the following ordering in terms of their association with values of τ_{corr}^{dip} and τ_{corr}^{OH} :



Interestingly, this trend exactly aligns with what we discovered in our previous study⁶⁰ about the degree of disorder of water orientations around negatively charged DND-COOHs. More specifically, we observed that water in NaCl and MgCl₂ solutions

organized themselves, respectively, in the most and the least randomly state around these DNDs.

2) We observe following trends for uncharged DNDs:

- a. τ_{corr}^{dip} values for water in the first hydration layer of DND-COOH and DND-NH₂ are almost identical in all salt solutions except for KCl solution. Moreover, they are 2 and 1.5 times larger than those of DND-H and DND-OH, respectively. In the case of water's OH bond reorientation relaxation, we have found the following ordering among DNDs:



We speculate that the driving factor behind this ordering is the nature of HBs between surfaces of these DNDs and water in the first hydration layer. In our previous work⁶⁰, we observed that the majority of the aforementioned water molecules point their dipole vector away from facets of the uncharged DND-COOH and thus they act as HB acceptors. In contrast, they orient their dipole towards surfaces of DND-OH and DND-NH₂ with zero net charge and become a HB donor. Consequently, OH bonds of water are more engaged with surfaces of the DND-OH and DND-NH₂ than those of DND-COOH, which leads to larger τ_{corr}^{oh} around the former.

- b. For water in the second hydration layer of DNDs with zero net charge, DND-H is associated with the largest values for τ_{corr}^{dip} and τ_{corr}^{oh} . It could be due to the weakened water-water HBs between the first and the second hydration layers around neutral DNDs with polar surface groups. Indeed, surfaces of these DNDs are decorated with moieties such as COOH, NH₂, or OH, which form HBs with water in the first hydration layer. Therefore, it drives the first layer water to break some of its HBs with water in the second hydration layer. In contrast, since the uncharged DND-H is hydrophobic, it drives water in the first hydration layer to form more HBs with water in the second hydration layer.
- 3) For charged DNDs, observed trends are a little bit more complicated, as discussed below:

- a. τ_{corr}^{dip} and τ_{corr}^{oh} corresponding to water in the first hydration layer are smallest for DND-H at all absolute charge values greater than zero. It can be attributed to the less constrained environment for water nearby DND-H, with non-polar surface characteristics, compared to DND-NH₂ and DND-COOH.
- b. There seems to be a competition between charged DND-COOH and DND-NH₂ particles. In Table 2, we have specified which of these DNDs has won the competition in terms of the largest value for each of τ_{corr}^{dip} and τ_{corr}^{oh} corresponding to a specific salt solution and $|q|$ (i.e., the absolute net charges on the DND). The results in Table 2 corresponds to the first hydration layer. This table clearly shows that positively charged DND-NH₂ dominates negatively charged DND-COOH in terms of the overall relaxation time for the reorientation of water dipole (i.e., τ_{corr}^{dip}) in the first hydration layer, whereas the reverse is true for τ_{corr}^{oh} . This observation can be attributed to NH₃⁺ and COO⁻ species that exist on surfaces of charged DND-NH₂ and DND-COOH,

respectively. While NH_3^+ acts as a HB donor to water and locks in its dipole, COO^- appears as a HB acceptor from water and hence constrains the reorientation of its OH bonds.

- c. There are few exceptions to the overall trend that we just detected in part b above. Indeed, τ_{corr}^{dip} is larger around DND-COOH than that around DND-NH₂ for $|q|$ values of 28 and 56 and in the salt solution of MgCl₂. The same is true for the case of $|q|=28$ and the salt solution of CaCl₂. On the other hand, at $|q|=28$ and in salt solutions of NaCl and CaCl₂, it takes longer for water around DND-NH₂ to relax its OH bond's initial orientation than that around DND-COOH. We attribute these observations to the significant ordered structure that Mg²⁺ and Ca²⁺ (though relatively with a lesser degree than Mg²⁺) ions impart onto their nearby water by constraining its dipole. Nevertheless, it appears that the strength of water's dipole lockdown imposed by NH₃⁺ groups of DND-NH₂ at $|q|=84$ is greater than what induced by Mg²⁺ ions surrounding DND-COOH at $|q|=84$.
- d. τ_{corr}^{dip} for water in the second hydration layer of charged DNDs exhibits the following trend. DND-NH₂ is associated with largest values for τ_{corr}^{dip} at each specific amount of surface charges, if either of NaCl or KCl salts exists in the solution. However, the replacement of either of salts by CaCl₂ or MgCl₂ salts causes the water in the second hydration layer around DND-COOH to experience the longest relaxation in the reorientation of its dipole, compared with other charged DNDs. This effect can be explained by the substantial constraints that Mg²⁺ or Ca²⁺ cations impose on the dipole vector of their surrounding water. We saw in our previous study⁵⁸ that the aforementioned constraints can go beyond the first hydration shell of Mg²⁺ or Ca²⁺.

Table 2. Comparison of charged DND-COOH and DND-NH₂ particles in different salt solutions and various net absolute charges on the DND ($|q|$) to determine which one has the dominant effect in slowing down reorientational dynamics of water's dipole and OH orientations in the DND's first hydration layer. The color of a cell specifies the dominant DND.

Salt Solution	τ_{corr}^{dip}			τ_{corr}^{oh}		
	$ q =28$	$ q =56$	$ q =84$	$ q =28$	$ q =56$	$ q =84$
KCl						
NaCl						
CaCl ₂						
MgCl ₂						

We now aim at digging deeper into mechanisms of the reorientational dynamics of water around DNDs by using the EWIC model as a guide. According to this model, on the one hand, the semi-angle θ_{tot} of the cone, in which water reorients, and its associated wobbling-in-a-cone (hereafter, wobbling) diffusion coefficient D_c represent the local constraints on water's reorientational dynamics. On the other hand, the diffusion coefficient D_m reflects more global restrictions for complete reorientational relaxation of water. In particular, as Tan *et al.* pointed out⁵², θ_{tot} , D_c , and D_m for water's OH reorientations reflect two underlying processes in the

dynamics of HB networks. The first two parameters reflect local motions within the HB network such as HB stretching or angular vibrations, without breaking HBs. However, the third parameter reveals rearrangements in the HB network in a more global sense. In fact, the more rigid or flexible local HBs are, the narrower or wider the cone of the wobbling water is. Thus, the smaller value of the cone's semi-angle θ_{tot} lends itself to the slower wobbling diffusion coefficient D_c and vice versa. However, D_m for water's OH is related to the overall structural rearrangements in the HB networks. Therefore, smaller D_m implies that it takes longer to break old HBs and form new ones.

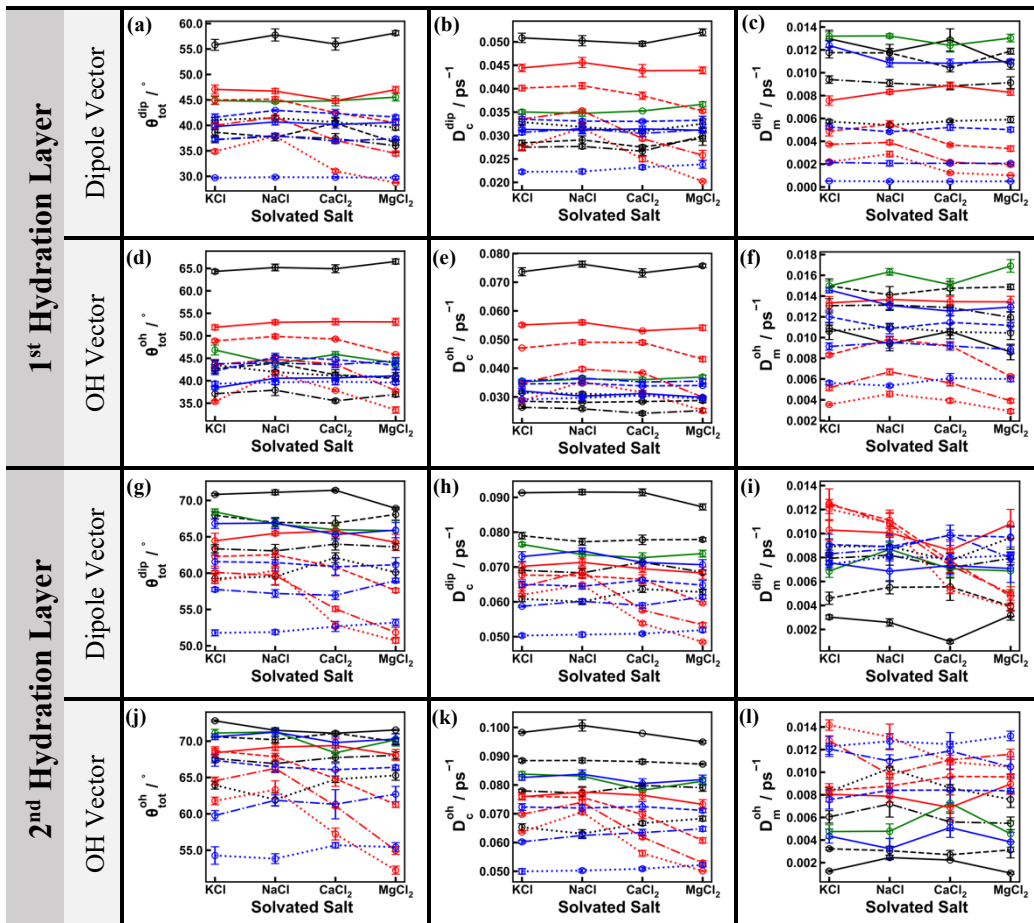


Figure 7. Parameters of EWIC model to describe the reorientational dynamics of water's dipole and OH orientations in two hydration layers of DNDs. θ_{tot} , D_c , and D_m denote the cone's semi-angle, wobbling diffusion coefficient, and rotational diffusion coefficient, respectively. Lines' styles and colors are the same as those in Figure 3.

With the aforementioned picture of the EWIC model in mind, we embark on analyzing the cone's semi-angle θ_{tot} , wobbling diffusion coefficient D_c , and rotational diffusion coefficient D_m , all of which are shown in Figure 7. Trends that appear in this figure not only support previous observations for τ_{corr}^{dip} and τ_{corr}^{oh} , but also reveal new insights that we have summarized below:

- 1) In both hydration layers, θ_{tot}^{dip} and θ_{tot}^{oh} as well as D_c^{dip} and D_c^{oh} corresponding to the uncharged DND–H have the highest values. In other words, the wobbling diffusion in the cone for water's dipole and OH orientations are the fastest nearby DND–H with zero net charge and the cone in which they locally rotate is the widest. It is expected due to the hydrophobic nature of this DND. In addition, since it is uncharged, there is no counterion nearby its surfaces to constrain orientational

degrees of freedom of water. However, D_m values corresponding to this DND reveal different reorientational behavior in two hydration layers. We observe that both dipole and OH orientations in the second hydration layer of the uncharged DND–H experience the slowest rotational diffusion out of the cone. It is in utter contrast to corresponding values of D_m in the first hydration layer. It could be due to the enhanced formation of HBs between water molecules in two hydration layers, which we had discussed before.

- 2) We observe an inverse relationship between the amount of the absolute net charges of DNDs and the values of θ_{tot} and D_c for both dipole and OH orientations in both hydration layers. Indeed, as the absolute net charges of DNDs increases, the values of these parameters decrease. Furthermore, results for DND–COOH reveal that there appears to be an interaction between the DND’s charge and the type of the cation in the salt solution. In particular, we can see that the wobbling diffusion coefficients D_c^{dip} and D_c^{oh} substantially drop for highly charged DND–COOH solvated in CaCl_2 and MgCl_2 solutions.
- 3) For charged DNDs, we observe noticeable differences for values of D_m in the first and second hydration layers around different DNDs, which are listed below:
 - a. In the first hydration layer around all charged DNDs, both D_m^{dip} and D_m^{oh} decrease with an increase in the DND’s net charges.
 - b. In contrast, when the DNDs’ absolute net charges increase, so do values of D_m^{dip} and D_m^{oh} for water in the second hydration layer of DNDs. However, there are few exceptions to this pattern. First, D_m^{dip} values for water in the second hydration layer of all negatively charged DND–COOH solvated in CaCl_2 and MgCl_2 salt solutions are smaller compared with the corresponding values of the uncharged DND–COOH. Second, in the same salt solutions just mentioned, water’s OH vector undergoes slower out of the cone rotational diffusion in the second hydration layer of DND–COOH with -84 charges than that of DND–COOH with -56 charges. Both of these exceptions can be attributed to the substantially constrained hydration shells around Ca^{2+} and Mg^{2+} cations that accumulate around negatively charged DND–COOH particles.

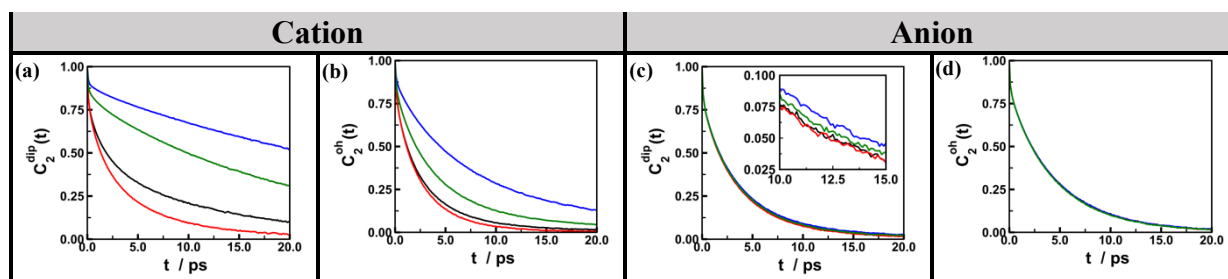


Figure 8. RCFs of dipole and OH orientations of water in the first hydration shell of constituent cation and anion of four different salts – KCl (red line), NaCl (black line), CaCl_2 (green line), MgCl_2 (blue line) – that are solvated in the aqueous solution of the neutral DND–H.

The influence of cations on the reorientational dynamics of water nearby DND–COOH, which we observed above, motivated us to study the same phenomena in the first hydration shell of ions themselves. For this purpose, we calculated RCFs for dipole and OH orientations of water

in the first hydration shell of cations and Cl^- anion in the salt solutions of the neutral DND–H. We have demonstrated the results in Figure 8. It is apparent from the decay rate of RCFs in Figure 8 (a-b) that cations slow down the reorientational dynamics of water’s dipole moment more intensely than that of its OH vector. The slowdown appears to be more pronounced around the divalent cations than that around the monovalent ones. Conversely, the decay rates of RCFs in Figure 8(c-d) around Cl^- anion seem to be almost identical for both water orientations, although some minor differences exist in RCFs for the dipole vector in four different Cl^- containing salt solutions.

To further elucidate the trends that we observed in Figure 8, we have fitted the tri-exponential function, which is used in the EWIC model, to the corresponding RCFs. The resulting four parameters of this model are shown in Figure 9 for both water orientations and are listed in the SI (Table S.22 and Table S.23). There are a couple of interesting trends in Figure 9 that we note below.

First, Figure 9(a, e) show that the overall relaxation time for dipole vector reorientations around K^+ , Na^+ , Ca^{2+} , and Mg^{2+} cations are, respectively, 1.5, 2.3, 3.6, and 3.9 times as long as the corresponding values for OH vector. Furthermore, we observe the following ordering in the overall reorientational relaxation time for both water orientations around cations, which follows the Hofmeister series:



Interestingly, this is exactly the same ordering we found elsewhere⁶⁰ for the peak intensity of probability distributions of angles that are formed between each of dipole and OH orientations and the line connecting each of the corresponding cations to the nearby water oxygen atoms. In addition, this trend is in good agreement with findings of Shattuck *et al.*⁶ that small, multivalent ions influence the dynamics of the nearby water molecules more profoundly than the large, monovalent ions do. This effect is linked to the higher charge density of the former ions, which in turn they establish stronger electric fields in their surroundings. The strong electric field of Mg^{2+} and Ca^{2+} can be sensed by even more distant water molecules, in contrast to larger, monovalent ions whose influences are mainly restricted to their first hydration shell.

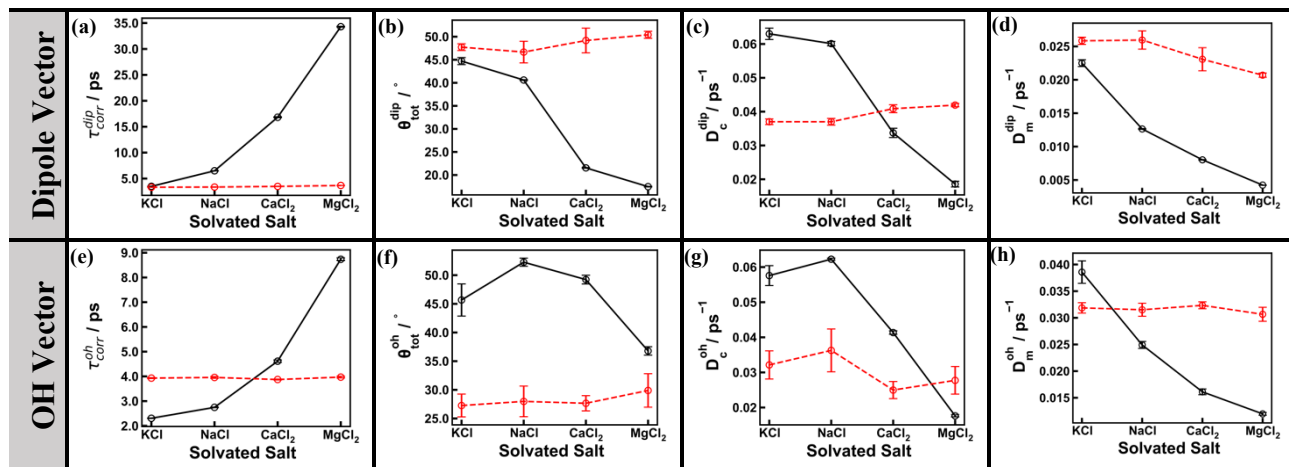


Figure 9. Same as Figure 7, but for water in the first hydration shell of constituent cation (black solid line) and anion (red dashed line) of four different salts (KCl, NaCl, CaCl₂, MgCl₂) that are solvated in the aqueous solution of the neutral DND–H.

Second, the total semi-angle of the cone for the dipole vector of the wobbling water around Mg^{2+} is 17.5° , which is the smallest compared with other cations. Indeed, it is almost 2.6 smaller than the corresponding value for the K^+ cation. The corresponding values for Na^+ and Ca^{2+} are 40.6° and 21.5° , respectively. Furthermore, Figure 9(c) reveals that the wobbling diffusion of the dipole vector of water around Ca^{2+} and Mg^{2+} cations is much slower than that around K^+ and Na^+ cations. These results show that the wobbling motion of water's dipole in the immediate surrounding of the divalent cations is much more restricted than that of the monovalent ones.

Third, results in Figure 9(f, g) also show more substantially restricted wobbling motion for water's OH vector around Mg^{2+} cation relative to other cations. However, we observe this kind of motion of OH vector around K^+ is more restricted than that around Na^+ , whereas we saw the reverse behavior for the dipole vector in Figure 9(b, c). The reason behind this observation will be discussed in more details later in this paper.

Four, the rotational diffusion coefficients D_m^{dip} and D_m^{oh} shown in Figure 9(d, h) follow the same ordering, yet in the reverse direction, that we presented for τ_{corr}^{dip} and τ_{corr}^{oh} before. These results together with what we observed before for D_c^{dip} and D_c^{oh} lead us to conclude that the reorientation of water's dipole and OH vectors around Ca^{2+} and more notably Mg^{2+} cations are extremely restricted both in their immediate vicinity and further away from them.

Five, values of τ_{corr}^{dip} around the Cl^- anion in KCl , NaCl , CaCl_2 , and MgCl_2 solutions are, respectively, 3.3, 3.4, 3.5, and 3.7 ps. The corresponding values for τ_{corr}^{oh} are 3.9, 4.0, 3.9, and 4.0 ps, respectively. Thus, as we also saw in Figure 8(c), the overall reorientational relaxations of the dipole vector around the Cl^- anion in CaCl_2 and MgCl_2 solutions are slightly larger than the corresponding values in KCl and NaCl solutions. Figure 9(d) also somehow reflects this trend, where the rotational diffusion of the dipole vector around Cl^- anion in CaCl_2 and MgCl_2 solutions is slower than that in other two solutions. Due to the nature of the rotational diffusion coefficient D_m , this effect can be ascribed to the fact that Mg^{2+} and Ca^{2+} (to a lesser degree) can restrict the rotation of water's dipole in larger distances away from themselves relative to two other cations.

Six, averaged over all salt solutions, τ_{corr}^{oh} of water around Cl^- anion is 13% larger than its τ_{corr}^{dip} around Cl^- . We attribute this difference to the HB between Cl^- and water, which thereby constrains the reorientation of water's OH bond. This statement is also supported by θ_{tot}^{dip} and θ_{tot}^{oh} values in Figure 9(b, f), where the latter is almost 50% smaller than the former. That is, constraints induced by Cl^- -water HB make the wobbling motion of water's OH bond take place in a smaller cone than that of its dipole moment.

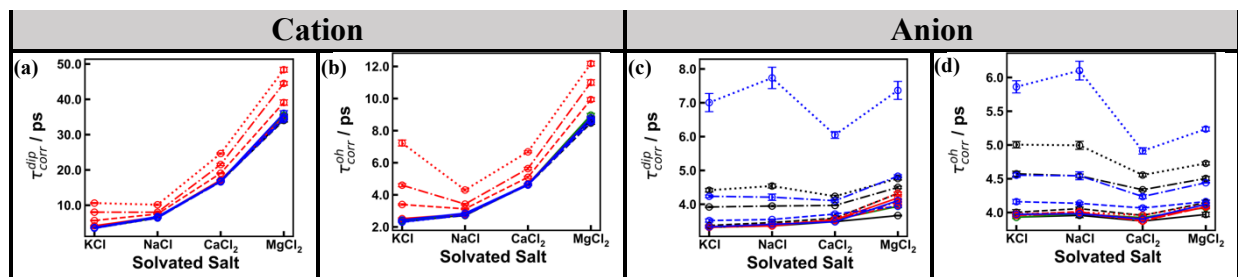


Figure 10. Correlation time of RCFs for dipole and OH orientations of water in the first hydration shell of constituent cation and anion of four different salts (KCl , NaCl , CaCl_2 , MgCl_2) that are solvated in the aqueous solution of different DNDs. DNDs are differentiated by different line styles and colors, which are explained in Figure 3.

In Figure 10, we have demonstrated the correlation time of RCFs for water orientations around ions (see SI, Table S.24 to Table S.39 for numerical values). These are different from what we presented in Figure 9 in the sense that Figure 10 also includes results from salt solutions of highly charged DNDs. More specifically, Figure 10 shows enhanced reorientational relaxations of both water orientations around ions in solutions of highly charged DNDs compared with those in uncharged DND solutions. For instance, both τ_{corr}^{dip} and τ_{corr}^{oh} values for water around cations in the solution of DND-COOH with -84 charges are noticeably larger than those in the solution of the neutral DND-COOH (see Figure 10(a)). In fact, high concentrations of oppositely charged ions are adsorbed onto the hydration layers of the DND in the former, whereas majority of ions reside further away from the DND's surfaces in the latter.

It is worthwhile to further investigate the aforementioned differences that we observe in the correlation times shown in Figure 10. These differences can be attributed to two factors: (1) the cooperation between surfaces of charged DNDs and interfacial accumulated counterions, (2) relatively high concentrations of counterions in the surrounding of charged DNDs. Prior studies^{6,56,71-73} support the likelihood of both factors, though their effects are not necessarily additive. In particular, Tielrooij *et al.* showed that cations and anions act cooperatively with each other and also with the surrounding species (such as polar functional groups on nanoparticles).³² Depending on the strength of ionic hydrations, the cooperative interactions can manifest different effects on the reorientational dynamics of the nearby water.

We have schematically demonstrated in Figure 11 how cooperative hydration by interfacial counterions and DNDs' charged surface groups manifest themselves in the first hydration layer of DNDs. In the case of positively charged DND-NH₂ solutions, Cl⁻ counterions accumulate in the proximity of DND's NH₃⁺ functional groups. Thereby, on the one hand, the interfacial water molecules act as hydrogen acceptors and form HBs with NH₃⁺ moieties as hydrogen donors, which leads to constraining the rotation of water's dipole vector. On the other hand, some of these water molecules donate a hydrogen to Cl⁻ ions and form HBs with them. Thus, the anions constrain the rotational motion of water's OH bond. In the case of positively charged DND-H solutions, although water does not form HBs with H atoms on DND's surfaces, water's dipole is still constrained by H atoms. However, this constraint is looser than what we described above for DND-NH₂ solutions.

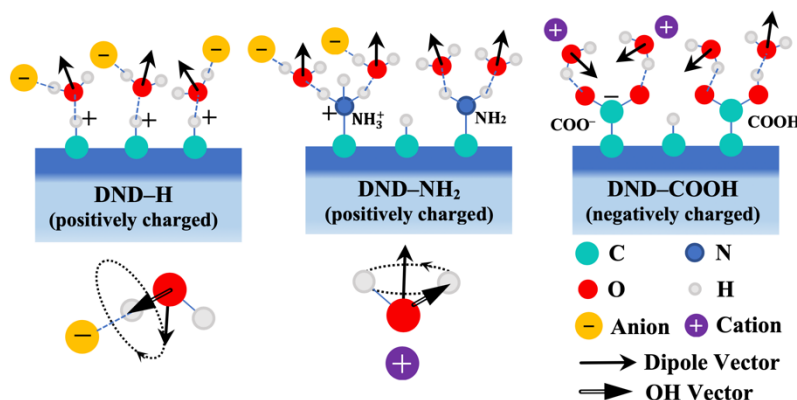


Figure 11. A schematic diagram that shows how DND's charged group and the adsorbed counterion on DND' surface can cooperatively influence reorientational dynamics of water. It can manifest in multiple directions, provided that both counterion and DND's charged group have high charge densities. (a)-(c) the first hydration layer of three different charged DNDs, (d) shows that an anion constrains water's OH bond, while its in the first hydration shell of anion, where water's OH bond is constrained by anion.

The cooperative hydration in the first hydration layer of negatively charged DND–COOHs is governed by a different mechanism. The COO[−] groups on these DNDs attract cations, which depending on their ionic strengths might be either physically adsorbed on those groups or be separated from those groups by a layer of water. Then, on the one hand, the adsorbed cations lock in the rotation of the interfacial water’s dipole vector. On the other hand, some of water molecules in the hydration shell of these cations donate HBs to COO[−] groups, which in turn results in constraining the OH bond of those water molecules.

4 Conclusion

We have performed MD simulations to study dynamics of the interfacial water in the aqueous salt solutions of DNDs. The goal is to determine how various surface chemistries of DNDs, on the one hand, and ions with different water affinities, on the other hand, influence the translational and rotational motion of water nearby surfaces of DNDs.

We have calculated the self-diffusion coefficient of water, as a signature of its translational mobility, in the whole hydration shell of DNDs from the slope of the MSD vs time plots. We have also developed a multiple regression model to verify if there are any statistically significant associations between the self-diffusion coefficient and various factors in our simulations. These factors include the type of surface functionalization on DNDs, the net charge of DNDs, and the type of solvated salt. Care has been taken to include interactions between these factors in our model. Our model shows significant impacts of all of these factors on the mobility of DNDs’ interfacial water, although their degree of influence varies under different conditions. Among all uncharged DNDs, carboxylated DND (DND–COOH) shows the largest slowdown effect on the mobility of the interfacial water, while water nearby the hydrogenated DND (DND–H) experiences the fastest translational motion. The former is explained by the stronger hydrogen bonding between the DND–COOH surfaces and the interfacial water compared with other DNDs, whereas the latter is attributed to the hydrophobicity of DND–H. Furthermore, we have observed that as the absolute net charge of DNDs increases, so does the DNDs’ retardation effect on the interfacial water mobility. We ascribe this effect to two interrelated factors: 1) constrained rotational dynamics of the interfacial water, 2) stronger DND–water HBs as a result of the addition of charged polar groups to DND surfaces. The second factor itself also contributes to the first factor. In addition, our regression model shows that there is a statistically significant interaction between the type of the cation in the solution and the amount of DND’s charges in solutions of charged carboxylated DNDs. In particular, we have observed $K^+ < Na^+ < Ca^{2+} < Mg^{2+}$ ordering, in terms of the degree of slowdown in the mobility of water in the proximity of the negatively charged DND–COOH, which is solvated in the corresponding chloride solution of these cations. This ordering, which concurs with Hofmeister series, also agrees with experimental observations^{74,75}. The significant reduction in the mobility of water associated with divalent cations has been ascribed to their high charge densities⁹, which results in the formation of strongly bound hydration shell around them. This is also confirmed by substantially higher residence time of water in the first hydration shell of divalent cations than that of monovalent cations.⁶⁰ Consequently, divalent cations carry with themselves their strongly bound water cage^{31,76,77}, as they move around in the hydration shell of negatively charged DND–COOH. Thereby, it entails the exertion of hydrodynamic friction by the surrounding water molecules. Thus, it eventually leads to significant reduction in the overall mobility of the interfacial water surrounded by Ca²⁺ or Mg²⁺ cations.

We now turn into summarizing our important findings in regard to reorientational dynamics of DNDs’ interfacial water. For this purpose, we have presented reorientational

correlation functions (RCF) for water's dipole and OH orientations in three hydration layers around DNDs. These hydration layers are defined based on the minima of density plots that we presented in our previous studies⁶⁰. Reorientational dynamics of water in the first two hydration layers are distinct from that of the last one, which is closer to the bulk region. In the former, we have observed that RCFs for both water orientations display three distinct reorientational relaxation modes. The three relaxations modes involve a fast, sub-picosecond decay followed by relaxation on ~ 1 -3 picosecond time scale and subsequently a slower relaxation on 10s-100s of picoseconds time scale. However, the RCF in the third hydration layer only displayed the aforementioned first and second relaxation modes, which is similar to what has been reported for bulk water⁵².

We have employed the extended wobbling-in-a-cone (EWIC) model to characterize RCF decays in the two closest hydration layers to DNDs' surfaces and thereby to elucidate the mechanism governing the rotational dynamics of the interfacial water. In this model, the first and second RCF relaxations correspond to librational and wobbling diffusion in hypothetical cones and the last slower relaxation is related to the rotational diffusion of the whole frame of water, which leads to the complete orientational randomization. Our results show that the positively charged DND-NH₂ and the negatively charged DND-COOH more substantially influence the orientational dynamics of water in their first hydration layers, compared with other DNDs. In general, in the first hydration layer, the former more predominantly retards the rotational dynamics of water's dipole, while the latter has dominant effects on slowing down the dynamics of water's OH rotation. We attribute these effects to HBs that NH₃⁺ on DND-NH₂ and COO⁻ on DND-COOH form with the interfacial water. The former is a hydrogen donor and hence lock in the rotation of water's dipole, whereas the latter is a hydrogen acceptor and thus constrains the reorientation of water's OH bond.

Similar to the translational dynamics, we have also observed specific cation effects on the rotational dynamics of both water's orientations in hydration layers of negatively charged DND-COOH. In this regard, we have learned that cations can be ranked as Na⁺ < K⁺ < Ca²⁺ < Mg²⁺ and Na⁺ < Ca²⁺ < K⁺ < Mg²⁺. These rankings reflect the degree of slowdown in the orientational dynamics of, respectively, dipole and OH vectors of water in the first hydration layer of charged DND-COOH. Since water is relatively weakly bound to K⁺ compared with other cations, it can form HBs with neighboring moieties (either water or functional groups on DND-COOH). Thus, it explains why water's OH reorientation is more constrained in the presence of K⁺ than that of Na⁺ and Ca²⁺ cations. It also agrees well with experimental observations⁶ that small charge density cations are structure-makers outside of their first hydration shell. However, Mg²⁺ binds water so tightly to its hydration shell that both water orientations are substantially constrained.

Our observations have led us to put forward a model for the reorientational dynamics of water hydrating charged DNDs that are surrounded by oppositely charged ions. In this model, which has been depicted in Figure 11, water hydrates charged DNDs in cooperation with adsorbed counterions. Thereby, the charged and polar functional groups on DNDs lock in either of water's dipole or OH orientations and counterions constrain the other orientation which has been pushed away from DNDs' surfaces. We suggest that the effect of the charged DND-counterion cooperative hydration on the dynamics of the interfacial water depends on three factors. These factors, which have also been reported in other studies^{9,32}, are the charge density of counterions, the concentration of counterions, and the strength of DND-water HB. We have observed the manifestations of the first two factors in both translational and reorientational dynamics of the interfacial water around negatively charged DND-COOH, surrounded by positively charged

counterions. In particular, Mg^{2+} with its strongly bound and highly immobilized hydration shells, imparted the slowest dynamics in the interfacial water, compared with other cations. Interestingly, higher concentration of Mg^{2+} reinforced this effect. The role of the third factor can be explained by energy cost associated with breaking the HB between the interfacial water and the DND's surface polar groups. We particularly observed the effect of this factor in the substantially retarded dipolar reorientational dynamics of water close to the DND covered with 84 NH_3^+ groups.

In summary, we have found that DNDs in cooperation with solvated ions have substantial impacts on both translational and rotational dynamics of DNDs' interfacial water. These results have implications for the dynamics of hydrogen bonding network of water around DNDs, which have significant impacts on performance of DNDs as fluorescent agents in bioimaging applications⁴⁶. In addition, our study paves the way to further investigate how the slowdown of the interfacial water's translational and rotational dynamics play a role in the colloidal stability of aqueous solution of DNDs.

References

1. Brini, E. *et al.* How Water's Properties Are Encoded in Its Molecular Structure and Energies. *Chem. Rev.* **117**, 12385–12414 (2017).
2. Luzar, A. & Chandler, D. Hydrogen-bond kinetics in liquid water. *Nature* **379**, (1996).
3. Laage, D., Stirnemann, G., Sterpone, F., Rey, R. & Hynes, J. T. Reorientation and Allied Dynamics in Water and Aqueous Solutions. *Annu. Rev. Phys. Chem.* **62**, 395–416 (2011).
4. Tielrooij, K. J., Van Der Post, S. T., Hunger, J., Bonn, M. & Bakker, H. J. Anisotropic water reorientation around ions. *J. Phys. Chem. B* **115**, 12638–12647 (2011).
5. Kaiser, A., Ritter, M., Nazmutdinov, R. & Probst, M. Hydrogen Bonding and Dielectric Spectra of Ethylene Glycol–Water Mixtures from Molecular Dynamics Simulations. *J. Phys. Chem. B* **120**, 10515–10523 (2016).
6. Shattuck, J., Shah, P., Erramilli, S. & Ziegler, L. D. Structure Making and Breaking Effects of Cations in Aqueous Solution: Nitrous Oxide Pump–Probe Measurements. *J. Phys. Chem. B* **120**, (2016).
7. Mancinelli, R., Botti, A., Bruni, F., Ricci, M. A. & Soper, A. K. Perturbation of water structure due to monovalent ions in solution. *Phys. Chem. Chem. Phys.* **9**, 2959–2967 (2007).
8. Burris, P. C., Laage, D. & Thompson, W. H. Simulations of the infrared, Raman, and 2D-IR photon echo spectra of water in nanoscale silica pores. *J. Chem. Phys.* **144**, 194709 (2016).
9. Stirnemann, G., Wernersson, E., Jungwirth, P. & Laage, D. Mechanisms of Acceleration and Retardation of Water Dynamics by Ions. *J. Am. Chem. Soc.* **135**, 11824–11831 (2013).
10. Gengeliczki, Z., Rosenfeld, D. E. & Fayer, M. D. Theory of interfacial orientational relaxation spectroscopic observables. *J. Chem. Phys.* **132**, (2010).
11. Yoosefian, M., Karimi-Maleh, H. & Sanati, A. L. A theoretical study of solvent effects on the characteristics of the intramolecular hydrogen bond in Droxidopa. *J. Chem. Sci.* **127**, 1007–1013 (2015).
12. Alizadeh, M., Azar, P. A., Mozaffari, S. A., Karimi-Maleh, H. & Tamaddon, A. M. A DNA Based Biosensor Amplified With ZIF-8/Ionic Liquid Composite for Determination of Mitoxantrone Anticancer Drug: An Experimental/Docking Investigation. *Front. Chem.* **8**, 1–10 (2020).

13. Harpham, M. R., Ladanyi, B. M., Levinger, N. E. & Herwig, K. W. Water motion in reverse micelles studied by quasielastic neutron scattering and molecular dynamics simulations. *J. Chem. Phys.* **121**, 7855–7868 (2004).
14. Zhao, W., Moilanen, D. E., Fenn, E. E. & Fayer, M. D. Water at the surfaces of aligned phospholipid multibilayer model membranes probed with ultrafast vibrational spectroscopy. *J. Am. Chem. Soc.* **130**, 13927–13937 (2008).
15. Srivastava, A. & Debnath, A. Hydration dynamics of a lipid membrane: Hydrogen bond networks and lipid-lipid associations. *J. Chem. Phys.* **148**, 094901–094901 (2018).
16. Capponi, S., White, S. H., Tobias, D. J. & Heyden, M. Structural Relaxation Processes and Collective Dynamics of Water in Biomolecular Environments. *J. Phys. Chem. B* **123**, 480–486 (2018).
17. Laage, D., Elsaesser, T. & Hynes, J. T. Water Dynamics in the Hydration Shells of Biomolecules. *Chem. Rev.* **117**, 10694–10725 (2017).
18. Ball, P. Water as an active constituent in cell biology. *Chem. Rev.* **108**, 74–108 (2008).
19. Fogarty, A. C. & Laage, D. Water Dynamics in Protein Hydration Shells: The Molecular Origins of the Dynamical Perturbation. *J. Phys. Chem. B* **118**, 53 (2014).
20. Brovchenko, I. & Oleinikova, A. Which properties of a spanning network of hydration water enable biological functions? *ChemPhysChem* **9**, 2695–2702 (2008).
21. Oleinikova, A., Smolin, N. & Brovchenko, I. Influence of water clustering on the dynamics of hydration water at the surface of a lysozyme. *Biophys. J.* **93**, 2986–3000 (2007).
22. Levy, Y. & Onuchic, J. N. Water Mediation in Protein Folding and Molecular Recognition. *Annu. Rev. Biophys. Biomol. Struct.* **35**, 389–415 (2006).
23. Fenimore, P. W., Frauenfelder, H., McMahon, B. H. & Parak, F. G. Slaving: Solvent fluctuations dominate protein dynamics and functions. *PNAS* **99**, 16047–16051 (2002).
24. Fogarty, A. C., Duboué-Dijon, E., Sterpone, F., Hynes, J. T. & Laage, D. Biomolecular hydration dynamics: A jump model perspective. *Chem. Soc. Rev.* **42**, 5672–5683 (2013).
25. Hofmeister, F. Zur Lehre von der Wirkung der Salze. *Arch. für Exp. Pathol. und Pharmakologie* **24**, 247–260 (1888).
26. Zajforoushan Moghaddam, S. & Thormann, E. The Hofmeister series: Specific ion effects in aqueous polymer solutions. *J. Colloid Interface Sci.* **555**, 615–635 (2019).
27. Yue, S. & Panagiotopoulos, A. Z. Dynamic properties of aqueous electrolyte solutions from non-polarisable, polarisable, and scaled-charge models. *Mol. Phys.* **117**, 3538–3549 (2019).
28. Collins, K. D. Ions from the Hofmeister series and osmolytes: Effects on proteins in solution and in the crystallization process. *Methods* **34**, 300–311 (2004).
29. Marcus, Y. Effect of ions on the structure of water: Structure making and breaking. *Chem. Rev.* **109**, 1346–1370 (2009).
30. Smith, J. D., Saykally, R. J. & Geissler, P. L. The effects of dissolved halide anions on hydrogen bonding in liquid water. *J. Am. Chem. Soc.* **129**, 13847–13856 (2007).
31. Choppin, G. R. & Buijs, K. Near-Infrared Studies of the Structure of Water. II. Ionic Solutions. *J. Chem. Phys.* **39**, 2042–2050 (1963).
32. Tielrooij, K. J., Garcia-Araez, N., Bonn, M. & Bakker, H. J. Cooperativity in Ion Hydration. *Science* vol. 328 1006–1009 (2010).
33. Xie, W. J. & Gao, Y. Q. Ion cooperativity and the effect of salts on polypeptide structure - A molecular dynamics study of BBA5 in salt solutions. *Faraday Discuss.* **160**, 191–206

- (2013).
34. Kitadai, N. *et al.* Effects of ions on the OH stretching band of water as revealed by atr-ir spectroscopy. *J. Solution Chem.* **43**, 1055–1077 (2014).
 35. Hribar, B., Southall, N. T., Vlachy, V. & Dill, K. A. How Ions Affect the Structure of Water. *J Am Chem Soc.* **124**, 12302–12311 (2002).
 36. Lin, Y. W. *et al.* Co-delivery of paclitaxel and cetuximab by nanodiamond enhances mitotic catastrophe and tumor inhibition. *Sci. Rep.* **7**, (2017).
 37. Wang, P., Su, W. & Ding, X. Control of nanodiamond-doxorubicin drug loading and elution through optimized compositions and release environments. *Diam. Relat. Mater.* **88**, 43–50 (2018).
 38. Siafaka, P. I., Üstündağ Okur, N., Karavas, E. & Bikiaris, D. N. Surface modified multifunctional and stimuli responsive nanoparticles for drug targeting: Current status and uses. *Int. J. Mol. Sci.* **17**, (2016).
 39. Liu, K. K. *et al.* Covalent linkage of nanodiamond-paclitaxel for drug delivery and cancer therapy. *Nanotechnology* **21**, (2010).
 40. Saraf, J., Kalia, K., Bhattacharya, P. & Tekade, R. K. Growing synergy of nanodiamonds in neurodegenerative interventions. *Drug Discov. Today* **24**, 584–594 (2019).
 41. Prabhakar, N. & Rosenholm, J. M. Nanodiamonds for advanced optical bioimaging and beyond. *Curr. Opin. Colloid Interface Sci.* **39**, 220–231 (2019).
 42. Guo, Y., Li, S., Li, W., Moosa, B. & Khashab, N. M. The Hofmeister effect on nanodiamonds: How addition of ions provides superior drug loading platforms. *Biomater. Sci.* **2**, 84–88 (2014).
 43. Zhu, Y. *et al.* Excessive sodium ions delivered into cells by nanodiamonds: Implications for tumor therapy. *Small* **8**, 1771–1779 (2012).
 44. Li, J. *et al.* Nanodiamonds as intracellular transporters of chemotherapeutic drug. *Biomaterials* **31**, 8410–8418 (2010).
 45. Huang, H., Pierstorff, E., Osawa, E. & Ho, D. Active nanodiamond hydrogels for chemotherapeutic delivery. *Nano Lett.* **7**, 3305–3314 (2007).
 46. Vervald, A. M. *et al.* Relationship Between Fluorescent and Vibronic Properties of Detonation Nanodiamonds and Strength of Hydrogen Bonds in Suspensions. *J. Phys. Chem. C* **120**, 19375–19383 (2016).
 47. Chen, C., Li, W. Z., Song, Y. C., Weng, L. D. & Zhang, N. Concentration dependence of water self-diffusion coefficients in dilute glycerol-water binary and glycerol-water-sodium chloride ternary solutions and the insights from hydrogen bonds. *Mol. Phys.* **110**, 283–291 (2012).
 48. Choudhary, A. & Chandra, A. Anisotropic structure and dynamics of the solvation shell of a benzene solute in liquid water from ab initio molecular dynamics simulations. *Phys. Chem. Chem. Phys.* **18**, 6132 (2016).
 49. Fogarty, A. C., Duboué-Dijon, E., Laage, D. & Thompson, W. H. Origins of the non-exponential reorientation dynamics of nanoconfined water. *J. Chem. Phys.* **141**, 18–523 (2014).
 50. Duboué-Dijon, E. & Laage, D. Characterization of the Local Structure in Liquid Water by Various Order Parameters. *J. Phys. Chem. B* **119**, 8406–8418 (2015).
 51. Bhide, S. Y. & Berkowitz, M. L. The behavior of reorientational correlation functions of water at the water-lipid bilayer interface. *J. Chem. Phys.* **125**, (2006).
 52. Tan, H. S., Piletic, I. R. & Fayer, M. D. Orientational dynamics of water confined on a

- nanometer length scale in reverse micelles. *J. Chem. Phys.* **122**, (2005).
53. Debnath, A., Mukherjee, B., Ayappa, K. G., Maiti, P. K. & Lin, S. T. Entropy and dynamics of water in hydration layers of a bilayer. *J. Chem. Phys.* **133**, (2010).
 54. Yamada, S. A., Shin, J. Y., Thompson, W. H. & Fayer, M. D. Water Dynamics in Nanoporous Silica: Ultrafast Vibrational Spectroscopy and Molecular Dynamics Simulations. *J. Phys. Chem. C* **123**, 5790–5803 (2019).
 55. Yamada, S. A., Thompson, W. H. & Fayer, M. D. Water-anion hydrogen bonding dynamics: Ultrafast IR experiments and simulations. *J. Chem. Phys.* **146**, 234501 (2017).
 56. Post, S. T. V. Der & Bakker, H. J. The combined effect of cations and anions on the dynamics of water. *Phys. Chem. Chem. Phys.* **14**, 6280–6288 (2012).
 57. Saberi Movahed, F., Cheng, G. C. & Venkatachari, B. S. Atomistic simulation of thermal decomposition of crosslinked and non-crosslinked phenolic resin chains. in *42nd AIAA Thermophysics Conference* (2011).
 58. Brenner, D. *et al.* Nanodiamond-based Nanolubricants: Experiment and Modeling. in *Mater. Res. Soc. Symp. Proc* 1703 (2014). doi:10.1557/opl.2014.
 59. Su, L., Krim, J. & Brenner, D. W. Interdependent Roles of Electrostatics and Surface Functionalization on the Adhesion Strengths of Nanodiamonds to Gold in Aqueous Environments Revealed by Molecular Dynamics Simulations. *J. Phys. Chem. Lett.* **9**, 4396–4400 (2018).
 60. Saberi-Movahed, F. & Brenner, D. W. What drives adsorption of ions on surface of nanodiamonds in aqueous solutions? *arXiv:2102.09187 [physics.comp-ph]* (2021).
 61. Michaud-Agrawal, N., Denning, E. J., Woolf, T. B. & Beckstein, O. MDAAnalysis: A toolkit for the analysis of molecular dynamics simulations. *J. Comput. Chem.* **32**, 2319–2327 (2011).
 62. Gowers, R. J. *et al.* MDAAnalysis: A Python Package for the Rapid Analysis of Molecular Dynamics Simulations. in *Proc. Of The 15th Python In Science Conf. (SciPy 2016)* (2016).
 63. Gillen, K. T., Douglass, D. C. & Hoch, M. J. R. Self-diffusion in liquid water to -31°C. *J. Chem. Phys.* **57**, 5117–5119 (1972).
 64. Holz, M., Heil, S. R. & Sacco, A. Temperature-dependent self-diffusion coefficients of water and six selected molecular liquids for calibration in accurate 1H NMR PFG measurements. *Phys. Chem. Chem. Phys.* **2**, 4740–4742 (2000).
 65. Friant-Michel, P., Wax, J. F., Meyer, N., Xu, H. & Millot, C. Translational and Rotational Diffusion in Liquid Water at Very High Pressure: A Simulation Study. *J. Phys. Chem. B* **123**, 10025–10035 (2019).
 66. Laage, D. & Hynes, J. T. A Molecular Jump Mechanism of Water Reorientation. *Science* vol. 311 832–835 (2006).
 67. Laage, D. & Hynes, J. T. On the Molecular Mechanism of Water Reorientation. *J. Phys. Chem. B* **112**, 14230–14242 (2008).
 68. Yadav, S., Choudhary, A. & Chandra, A. A First-Principles Molecular Dynamics Study of the Solvation Shell Structure, Vibrational Spectra, Polarity, and Dynamics around a Nitrate Ion in Aqueous Solution. *J. Phys. Chem. B* **121**, 9032–9044 (2017).
 69. Samoilov, Y. A new approach to the study of hydration of ions in aqueous solutions. *Discuss. Faraday Soc.* **24**, 141–146 (1957).
 70. Collins, K. D. Charge Density-Dependent Strength of Hydration and Biological Structure. *Biophys. J.* **72**, 65–76 (1997).

71. Pastorczak, M., Van Der Post, S. T. & Bakker, H. J. Cooperative hydration of carboxylate groups with alkali cations. *Phys.Chem.Chem.Phys* **15**, 17767–17770 (2013).
72. Baul, U. & Vemparala, S. Ion hydration and associated defects in hydrogen bond network of water: Observation of reorientationally slow water molecules beyond first hydration shell in aqueous solutions of MgCl₂. *Phys. Rev. E* **91**, (2015).
73. Vila Verde, A. & Lipowsky, R. Cooperative slowdown of water rotation near densely charged ions is intense but short-ranged. *J. Phys. Chem. B* **117**, 10556–10566 (2013).
74. Muller, K. J. & Hertz, H. G. A Parameter as an Indicator for Water-Water Association in Solutions of Strong Electrolytes. *J. Phys. Chem.* **100**, 1256–1265 (1996).
75. Kim, J. S., Wu, Z., Morrow, A. R., Yethiraj, A. & Yethiraj, A. Self-diffusion and viscosity in electrolyte solutions. *J. Phys. Chem. B* **116**, 12007–12013 (2012).
76. Hartkamp, R. & Coasne, B. Structure and transport of aqueous electrolytes: From simple halides to radionuclide ions. *J. Chem. Phys.* **141**, (2014).
77. Omta, A. W., Kropman, M. F., Woutersen, S. & Bakker, H. J. Negligible Effect of Ions on the Hydrogen-Bond Structure in Liquid Water. *Science* vol. 301 347–349 (2003).

Supplementary Information (SI)

This section contains tables of parameters introduced in the main body of the paper for the translational and the reorientational motion of water around various detonation nanodiamonds (DNDs) and ions in aqueous solutions. In Section S.1, the 95% confidence interval (CI) for the average diffusion coefficient of water in the whole hydration shell of each distinct DND in a specific salt solution is presented. We have calculated the CI using the bootstrap percentile method¹, where the bootstrap distribution was obtained by resampling the initial sample data 10,000 times with replacement. We have computed the average value of all parameters in this appendix from five independent MD trajectories. Thus, the sample data for each distinct DND in a particular salt solution have five data points.

S.1. Translational dynamics

As it was mentioned in Section 2, the self-diffusion coefficient D is obtained from the slope of the Mean Square Displacement (MSD) vs. time plot. We estimated this slope from a linear regression model fitted to the plot. The Standard Error (SE) is provided in Table S.1–Table S.5. for the estimate of D corresponding to each of five independent MD trajectories.

Table S.1. The self-diffusion coefficient D of water in the whole hydration shell of DND–H with various surface chemistries. D_i ($i=1, 2, \dots, 5$) corresponds to the i th MD trajectory and D_{mean} is the average value. Values of D , SE, and CI are expressed in $10^{-9} \text{ m}^2 \cdot \text{sec}^{-1}$.

DND's Charge	Dissolved Salt	D_1 (SE)	D_2 (SE)	D_3 (SE)	D_4 (SE)	D_5 (SE)	D_{mean} (CI)
q = 0	KCl	2.45 (4.98E-3)	2.44 (3.71E-3)	2.46 (4.33E-3)	2.46 (4.52E-3)	2.44 (3.87E-3)	2.45 (2.442, 2.458)
	NaCl	2.45 (4.29E-3)	2.38 (3.71E-3)	2.41 (4.08E-3)	2.41 (3.61E-3)	2.44 (3.75E-3)	2.418 (2.398, 2.438)
	CaCl₂	2.32 (2.78E-3)	2.39 (3.37E-3)	2.39 (3.38E-3)	2.4 (3.75E-3)	2.37 (3.86E-3)	2.374 (2.346, 2.394)
	MgCl₂	2.37 (2.88E-3)	2.37 (3.44E-3)	2.34 (4.07E-3)	2.37 (3.34E-3)	2.39 (3.50E-3)	2.368 (2.352, 2.382)
q = +28	KCl	2.23 (4.75E-3)	2.22 (4.76E-3)	2.2 (4.30E-3)	2.21 (4.83E-3)	2.2 (5.44E-3)	2.212 (2.202, 2.222)
	NaCl	2.21 (4.94E-3)	2.25 (5.21E-3)	2.21 (5.70E-3)	2.19 (4.76E-3)	2.2 (4.98E-3)	2.212 (2.198, 2.232)
	CaCl₂	2.18 (4.59E-3)	2.16 (4.49E-3)	2.19 (4.93E-3)	2.17 (4.93E-3)	2.24 (5.11E-3)	2.188 (2.168, 2.214)
	MgCl₂	2.18 (4.24E-3)	2.14 (4.48E-3)	2.15 (4.27E-3)	2.23 (5.21E-3)	2.2 (4.40E-3)	2.18 (2.152, 2.208)
q = +56	KCl	2.14 (4.97E-3)	2.15 (6.08E-3)	2.15 (6.13E-3)	2.15 (5.50E-3)	2.17 (6.64E-3)	2.152 (2.144, 2.162)
	NaCl	2.13 (5.60E-3)	2.19 (5.66E-3)	2.13 (5.07E-3)	2.12 (5.19E-3)	2.13 (5.23E-3)	2.14 (2.124, 2.166)
	CaCl₂	2.11 (4.61E-3)	2.1 (4.54E-3)	2.11 (4.63E-3)	2.1 (4.76E-3)	2.11 (4.49E-3)	2.106 (2.102, 2.110)

	MgCl₂	2.09 (4.60E-3)	2.14 (5.33E-3)	2.13 (5.02E-3)	2.13 (5.24E-3)	2.1 (5.62E-3)	2.118 (2.100, 2.134)
q = +84	KCl	2.03 (6.13E-3)	2.05 (5.43E-3)	2 (5.79E-3)	2.03 (5.48E-3)	1.99 (5.39E-3)	2.02 (2.000, 2.038)
	NaCl	2.04 (5.41E-3)	2.02 (5.82E-3)	2 (5.00E-3)	2.02 (5.74E-3)	2.04 (5.88E-3)	2.024 (2.012, 2.036)
	CaCl₂	2.01 (5.44E-3)	2.03 (5.41E-3)	2.06 (5.52E-3)	2.02 (6.19E-3)	2 (5.48E-3)	2.024 (2.008, 2.044)
	MgCl₂	2 (4.99E-3)	1.98 (4.87E-3)	2 (5.39E-3)	2.05 (5.13E-3)	2.02 (5.03E-3)	2.01 (1.992, 2.032)

Table S.2. Same as Table S.1, but for the case of DND–NH₂.

DND's Charge	Dissolved Salt	D₁ (SE)	D₂ (SE)	D₃ (SE)	D₄ (SE)	D₅ (SE)	D_{mean} (CI)
q = 0	KCl	1.95 (5.85E-03)	1.93 (6.26E-03)	1.94 (5.47E-03)	1.98 (6.16E-03)	1.98 (6.36E-03)	1.956 (1.938, 1.974)
	NaCl	1.94 (7.02E-03)	1.93 (5.90E-03)	1.97 (6.56E-03)	1.91 (5.51E-03)	1.93 (5.51E-03)	1.936 (1.920, 1.954)
	CaCl₂	1.91 (5.94E-03)	1.92 (6.04E-03)	1.95 (6.23E-03)	1.95 (6.41E-03)	1.93 (6.00E-03)	1.932 (1.918, 1.946)
	MgCl₂	1.87 (6.09E-03)	1.92 (5.91E-03)	1.87 (5.37E-03)	1.9 (5.38E-03)	1.89 (6.15E-03)	1.89 (1.874, 1.906)
q = +28	KCl	1.99 (7.38E-03)	1.93 (6.12E-03)	1.94 (5.96E-03)	1.94 (6.89E-03)	1.93 (5.78E-03)	1.946 (1.932, 1.968)
	NaCl	1.96 (6.15E-03)	1.96 (5.94E-03)	1.95 (5.82E-03)	1.93 (6.13E-03)	1.91 (6.11E-03)	1.942 (1.924, 1.958)
	CaCl₂	1.92 (5.56E-03)	1.93 (6.41E-03)	1.91 (5.88E-03)	1.9 (6.34E-03)	1.88 (4.89E-03)	1.908 (1.892, 1.922)
	MgCl₂	1.91 (6.36E-03)	1.89 (5.74E-03)	1.92 (6.24E-03)	1.94 (5.41E-03)	1.9 (5.33E-03)	1.912 (1.898, 1.928)
q = +56	KCl	1.85 (6.51E-03)	1.85 (5.86E-03)	1.81 (5.29E-03)	1.87 (6.80E-03)	1.83 (4.90E-03)	1.842 (1.826, 1.858)
	NaCl	1.87 (6.15E-03)	1.85 (6.39E-03)	1.85 (5.78E-03)	1.84 (5.52E-03)	1.82 (5.75E-03)	1.846 (1.832, 1.860)
	CaCl₂	1.88 (6.36E-03)	1.86 (5.21E-03)	1.81 (5.09E-03)	1.84 (5.76E-03)	1.85 (6.03E-03)	1.848 (1.828, 1.868)
	MgCl₂	1.83 (5.49E-03)	1.81 (5.31E-03)	1.83 (6.33E-03)	1.81 (5.31E-03)	1.84 (5.65E-03)	1.824 (1.814, 1.834)
q = +84	KCl	1.68 (6.62E-03)	1.71 (6.30E-03)	1.66 (6.40E-03)	1.65 (5.67E-03)	1.68 (6.29E-03)	1.676 (1.658, 1.694)
	NaCl	1.67 (6.03E-03)	1.65 (5.11E-03)	1.7 (4.85E-03)	1.71 (6.10E-03)	1.68 (6.87E-03)	1.682 (1.664, 1.700)
	CaCl₂	1.66	1.66	1.69	1.67	1.66	1.668

		(5.76E-03)	(5.62E-03)	(6.38E-03)	(5.19E-03)	(5.53E-03)	(1.660, 1.680)
	MgCl₂	1.67 (5.42E-03)	1.68 (5.22E-03)	1.65 (5.65E-03)	1.66 (5.73E-03)	1.66 (5.42E-03)	1.664 (1.656, 1.674)

Table S.3. Same as Table S.1, but for the case of DND–COOH.

DND's Charge	Dissolved Salt	D_1 (SE)	D_2 (SE)	D_3 (SE)	D_4 (SE)	D_5 (SE)	D_{mean} (CI)
q = 0	KCl	1.9 (7.34E-03)	1.9 (8.11E-03)	1.87 (7.26E-03)	1.91 (6.81E-03)	1.85 (6.29E-03)	1.886 (1.866, 1.904)
	NaCl	1.86 (6.97E-03)	1.86 (6.45E-03)	1.84 (5.99E-03)	1.88 (6.49E-03)	1.88 (6.60E-03)	1.864 (1.852, 1.876)
	CaCl₂	1.84 (7.30E-03)	1.81 (6.65E-03)	1.82 (7.27E-03)	1.82 (6.06E-03)	1.86 (7.57E-03)	1.83 (1.816, 1.848)
	MgCl₂	1.84 (6.36E-03)	1.8 (6.99E-03)	1.83 (6.93E-03)	1.82 (6.28E-03)	1.84 (6.43E-03)	1.826 (1.812, 1.838)
q = -28	KCl	1.94 (6.73E-03)	1.92 (6.85E-03)	1.91 (6.64E-03)	1.89 (6.12E-03)	1.85 (6.48E-03)	1.902 (1.874, 1.926)
	NaCl	1.82 (5.99E-03)	1.86 (6.90E-03)	1.85 (6.53E-03)	1.9 (6.77E-03)	1.87 (6.65E-03)	1.86 (1.836, 1.882)
	CaCl₂	1.72 (6.06E-03)	1.73 (6.46E-03)	1.73 (6.06E-03)	1.74 (5.97E-03)	1.74 (6.31E-03)	1.732 (1.726, 1.738)
	MgCl₂	1.6 (5.52E-03)	1.6 (5.76E-03)	1.62 (6.04E-03)	1.58 (5.61E-03)	1.6 (6.17E-03)	1.6 (1.588, 1.612)
q = -56	KCl	1.83 (6.44E-03)	1.85 (7.76E-03)	1.83 (6.75E-03)	1.8 (6.06E-03)	1.84 (8.00E-03)	1.83 (1.814, 1.842)
	NaCl	1.8 (6.61E-03)	1.78 (7.22E-03)	1.81 (6.48E-03)	1.81 (6.42E-03)	1.77 (6.72E-03)	1.794 (1.780, 1.808)
	CaCl₂	1.61 (6.57E-03)	1.53 (6.55E-03)	1.57 (5.70E-03)	1.54 (6.04E-03)	1.56 (6.17E-03)	1.562 (1.540, 1.588)
	MgCl₂	1.34 (5.74E-03)	1.32 (4.95E-03)	1.31 (5.05E-03)	1.34 (4.83E-03)	1.36 (5.55E-03)	1.334 (1.318, 1.348)
q = -84	KCl	1.76 (6.23E-03)	1.8 (7.21E-03)	1.76 (6.56E-03)	1.79 (6.88E-03)	1.76 (6.81E-03)	1.774 (1.760, 1.790)
	NaCl	1.69 (6.60E-03)	1.68 (5.35E-03)	1.7 (6.95E-03)	1.67 (6.27E-03)	1.7 (6.73E-03)	1.688 (1.678, 1.698)
	CaCl₂	1.39 (5.69E-03)	1.39 (5.57E-03)	1.37 (5.32E-03)	1.38 (6.33E-03)	1.41 (5.78E-03)	1.388 (1.376, 1.400)
	MgCl₂	1.2 (5.01E-03)	1.19 (4.80E-03)	1.18 (4.68E-03)	1.21 (5.37E-03)	1.19 (5.03E-03)	1.194 (1.186, 1.204)

Table S.4. Same as Table S.1, but for the case of DND–OH.

DND's Charge	Dissolved Salt	D_1 (SE)	D_2 (SE)	D_3 (SE)	D_4 (SE)	D_5 (SE)	D_{mean} (CI)
q = 0	KCl	2.01	2.07	2.05	2.01	2.02	2.032

		(5.89E-03)	(7.01E-03)	(5.41E-03)	(4.80E-03)	(5.92E-03)	(2.012, 2.054)
	NaCl	2.04 (6.37E-03)	2 (5.72E-03)	2 (5.81E-03)	2 (5.18E-03)	2.01 (5.89E-03)	2.01 (2.000, 2.026)
	CaCl₂	2.02 (5.29E-03)	2 (6.45E-03)	1.98 (6.59E-03)	1.98 (5.73E-03)	1.98 (5.40E-03)	1.992 (1.980, 2.008)
	MgCl₂	1.93 (4.99E-03)	1.99 (5.89E-03)	1.98 (6.30E-03)	1.92 (5.34E-03)	1.96 (6.05E-03)	1.956 (1.932, 1.980)

Table S.5. Same as Table S.1, but for the case of the bulk water, which corresponds to the region outside the whole hydration shell of the neutral DND–H in different salt solutions.

Dissolved Salt	D_1 (SE)	D_2 (SE)	D_3 (SE)	D_4 (SE)	D_5 (SE)	D_{mean} (CI)
KCl	2.68 (1.26E-03)	2.67 (1.56E-03)	2.65 (1.56E-03)	2.66 (1.47E-03)	2.65 (1.46E-03)	2.662 (2.652, 2.672)
NaCl	2.65 (1.22E-03)	2.63 (1.50E-03)	2.62 (1.66E-03)	2.63 (1.32E-03)	2.65 (1.52E-03)	2.636 (2.626, 2.646)
CaCl₂	2.61 (1.61E-03)	2.56 (1.55E-03)	2.6 (1.38E-03)	2.59 (1.44E-03)	2.58 (1.60E-03)	2.588 (2.572, 2.602)
MgCl₂	2.53 (1.59E-03)	2.57 (1.38E-03)	2.58 (9.97E-04)	2.56 (1.20E-03)	2.57 (1.64E-03)	2.562 (2.546, 2.574)

S.2. Reorientational dynamics

In this section parameters of the Extended Wobble-In-Cone (EWIC) model for the reorientational dynamics of the dipole moment and OH bonds of water in the two closest hydration layers to the facets of DNDs as well as the first hydration shell of ions are presented. We defined the EWIC model in Section 2.2 to study the reorientational dynamics of water. The values throughout this section are averaged over the five independent MD trajectories. Due to the space limit, the bootstrapped CI for these point estimates is not presented here.

S.2.1. First hydration layer of DNDs

S.2.1.1. Water’s dipole reorientation parameters

Table S.6. The EWIC parameters for the dipole reorientations of water in the first hydration layer of DND–H with various surface chemistries.

DND’s Charge	Dissolved Salt	τ_{in}^{dip} / ps	τ_c^{dip} / ps	τ_m^{dip} / ps	τ_{corr}^{dip} / ps	θ_{tot}^{dip} / °	d_c^{dip} / ps⁻¹	d_m^{dip} / ps⁻¹
q = 0	KCl	0.10364	3.86686	13.10119	4.16814	55.81	0.05085	0.01297
	NaCl	0.10806	4.07464	14.35162	4.22332	57.75	0.05024	0.0118
	CaCl₂	0.10728	3.97407	13.2983	4.20704	55.97	0.0496	0.01287
	MgCl₂	0.10925	3.97346	15.67982	4.40647	58.14	0.05204	0.0107
q = +28	KCl	0.09897	4.0275	14.2902	7.86731	38.64	0.02842	0.01176
	NaCl	0.0783	3.79346	14.28877	8.0469	37.69	0.02906	0.01173
	CaCl₂	0.0997	4.4814	16.065	8.39383	40.43	0.02751	0.01044

	MgCl ₂	0.07724	3.57976	14.06563	8.14519	36.60	0.0294	0.01188
q = +56	KCl	0.09886	3.89898	17.83693	10.07563	37.17	0.0275	0.0094
	NaCl	0.10035	3.98535	18.4576	10.21093	37.85	0.02768	0.00909
	CaCl ₂	0.10198	4.09401	18.99653	10.61264	37.42	0.02665	0.00884
	MgCl ₂	0.06058	3.4492	18.57953	10.65996	36.00	0.02988	0.00913
q = +84	KCl	0.0833	3.85082	29.19301	14.01016	41.08	0.03287	0.00573
	NaCl	0.10213	4.02185	30.79973	14.5868	41.45	0.03183	0.00542
	CaCl ₂	0.1043	4.01204	28.93855	14.16938	40.63	0.03089	0.00577
	MgCl ₂	0.07845	3.66457	28.57006	14.40992	39.54	0.03251	0.0059

Table S.7. Same as Table S.6, but for the case of DND–NH₂.

DND's Charge	Dissolved Salt	$\tau_{in}^{dip} / \text{ps}$	τ_c^{dip} / ps	τ_m^{dip} / ps	$\tau_{corr}^{dip} / \text{ps}$	$\theta_{tot}^{dip} / ^\circ$	$d_c^{dip} / \text{ps}^{-1}$	$d_m^{dip} / \text{ps}^{-1}$
q = 0	KCl	0.09803	3.82421	13.53894	7.2417	39.76	0.03131	0.01238
	NaCl	0.10015	4.00659	15.435	7.96411	40.67	0.03116	0.01086
	CaCl ₂	0.10065	3.88216	15.48775	8.07627	40.16	0.03142	0.01083
	MgCl ₂	0.09974	3.98522	15.19604	7.88507	40.59	0.03112	0.01099
q = +28	KCl	0.08331	3.86859	31.98036	14.88264	41.61	0.03348	0.00525
	NaCl	0.10222	4.09615	34.64087	15.3588	42.93	0.03308	0.00483
	CaCl ₂	0.10453	4.01266	32.37021	14.63898	42.34	0.03301	0.00521
	MgCl ₂	0.08194	3.89342	33.47322	15.56957	41.64	0.03327	0.00502
q = +56	KCl	0.0751	3.49801	78.85178	41.216	37.22	0.03066	0.00214
	NaCl	0.08006	3.54086	88.90453	44.52133	37.97	0.03148	0.00207
	CaCl ₂	0.05796	3.475	82.16318	43.40347	36.92	0.03044	0.00207
	MgCl ₂	0.0948	3.45173	81.15085	42.16081	37.38	0.03127	0.00207
q = +84	KCl	0.07861	3.2298	331.2225	218.31221	29.70	0.02225	0.00052
	NaCl	0.07866	3.25566	413.62591	270.05705	29.83	0.02232	0.00049
	CaCl ₂	0.06179	3.11535	377.14295	247.59176	29.78	0.02323	0.00048
	MgCl ₂	0.06224	3.04579	368.90627	241.75343	29.74	0.02383	0.0005

Table S.8. Same as Table S.6, but for the case of DND–COOH.

DND's Charge	Dissolved Salt	$\tau_{in}^{dip} / \text{ps}$	τ_c^{dip} / ps	τ_m^{dip} / ps	$\tau_{corr}^{dip} / \text{ps}$	$\theta_{tot}^{dip} / ^\circ$	$d_c^{dip} / \text{ps}^{-1}$	$d_m^{dip} / \text{ps}^{-1}$
q = 0	KCl	0.0848	3.82421	22.39306	8.62504	47.06	0.04443	0.00756
	NaCl	0.08127	4.00659	20.06443	7.95922	46.73	0.0456	0.00833
	CaCl ₂	0.08073	3.88216	18.87747	8.06852	44.82	0.04384	0.00888
	MgCl ₂	0.10074	3.98522	20.22526	7.95827	47.01	0.04391	0.00828
q = -28	KCl	0.10496	3.86859	35.51699	14.11705	44.98	0.04012	0.00487
	NaCl	0.10283	4.09615	30.75229	12.39242	45.15	0.04064	0.0055
	CaCl ₂	0.09758	4.01266	45.49722	19.87256	42.48	0.03851	0.00368
	MgCl ₂	0.09316	3.89342	51.12286	23.88304	40.53	0.03525	0.00336
q = -56	KCl	0.09957	3.49801	44.89813	21.65666	40.00	0.03351	0.00373
	NaCl	0.10076	3.54086	43.15506	19.56906	41.61	0.03529	0.0039

	CaCl ₂	0.08986	3.475	77.60349	40.90907	37.06	0.02933	0.00217
	MgCl ₂	0.05823	3.45173	88.38432	50.54925	34.48	0.02579	0.00196
q = -84	KCl	0.08581	3.2298	77.15366	43.78132	34.88	0.02739	0.0022
	NaCl	0.07846	3.25566	60.41896	30.98359	37.87	0.03163	0.00288
	CaCl ₂	0.07862	3.11535	140.95671	89.58144	31.01	0.02495	0.00124
	MgCl ₂	0.07809	3.04579	164.48044	111.97313	28.74	0.02023	0.00102

Table S.9. Same as Table S.6, but for the case of DND–OH.

DND's Charge	Dissolved Salt	$\tau_{in}^{dip} / \text{ps}$	τ_c^{dip} / ps	τ_m^{dip} / ps	$\tau_{corr}^{dip} / \text{ps}$	$\theta_{tot}^{dip} / ^\circ$	$d_c^{dip} / \text{ps}^{-1}$	$d_m^{dip} / \text{ps}^{-1}$
q = 0	KCl	0.09979	4.13937	12.67506	5.95401	44.87	0.03504	0.0132
	NaCl	0.09902	4.1569	12.61647	5.98507	44.66	0.03472	0.01322
	CaCl ₂	0.0982	4.10773	13.58546	6.2971	44.82	0.03525	0.01239
	MgCl ₂	0.07922	4.04983	12.83891	5.89379	45.54	0.03666	0.01303

S.2.1.2. Water's OH reorientation parameters

Table S.10. The EWIC parameters for the OH reorientations of water in the first hydration layer of DND–H with various surface chemistries.

DND's Charge	Dissolved Salt	$\tau_{in}^{oh} / \text{ps}$	τ_c^{oh} / ps	τ_m^{oh} / ps	$\tau_{corr}^{oh} / \text{ps}$	$\theta_{tot}^{oh} / ^\circ$	$d_c^{oh} / \text{ps}^{-1}$	$d_m^{oh} / \text{ps}^{-1}$
q = 0	KCl	0.12142	3.11636	15.37138	3.19053	64.32	0.07364	0.01089
	NaCl	0.1201	3.03949	18.24148	3.32216	65.20	0.07629	0.00939
	CaCl ₂	0.12391	3.15439	16.08699	3.18378	64.92	0.07325	0.0106
	MgCl ₂	0.12711	3.11379	20.01955	3.33645	66.54	0.07573	0.00861
q = +28	KCl	0.10575	4.71667	11.24145	5.91147	42.65	0.02846	0.01498
	NaCl	0.10829	4.97156	12.01114	6.07143	43.90	0.0281	0.01411
	CaCl ₂	0.10084	4.48225	11.42689	6.14744	41.33	0.02836	0.01475
	MgCl ₂	0.082	4.29991	11.21921	6.18347	40.52	0.02874	0.01488
q = +56	KCl	0.10062	4.05743	12.94021	7.58367	37.12	0.02636	0.01307
	NaCl	0.08448	4.29602	12.79358	7.44502	37.91	0.02585	0.01313
	CaCl ₂	0.10051	4.08629	12.95827	7.96991	35.53	0.02427	0.01289
	MgCl ₂	0.10107	4.21205	14.05662	8.28868	36.95	0.02523	0.01195
q = +84	KCl	0.11139	4.38285	16.18658	7.74503	43.50	0.03151	0.01061
	NaCl	0.0887	4.21055	15.13697	7.72799	41.93	0.03105	0.01104
	CaCl ₂	0.10479	4.11304	15.89739	8.21487	41.11	0.03072	0.01054
	MgCl ₂	0.10641	4.26319	16.26784	8.42471	40.89	0.02948	0.01045

Table S.11. Same as Table S.10, but for the case of DND–NH₂.

DND's Charge	Dissolved Salt	$\tau_{in}^{oh} / \text{ps}$	τ_c^{oh} / ps	τ_m^{oh} / ps	$\tau_{corr}^{oh} / \text{ps}$	$\theta_{tot}^{oh} / ^\circ$	$d_c^{oh} / \text{ps}^{-1}$	$d_m^{oh} / \text{ps}^{-1}$
q = 0	KCl	0.06099	3.52571	11.44787	6.51489	38.40	0.03211	0.01458
	NaCl	0.10326	4.08567	12.78403	6.86232	40.56	0.03025	0.0131

	CaCl ₂	0.10136	3.98114	13.35112	7.09269	40.62	0.0312	0.01255
	MgCl ₂	0.10457	4.2332	12.95901	6.86546	41.10	0.02985	0.01293
q = +28	KCl	0.0857	3.83243	14.00856	7.02776	42.13	0.03452	0.01201
	NaCl	0.11085	4.23908	15.50304	7.03958	45.30	0.0348	0.01087
	CaCl ₂	0.11049	4.26547	14.75362	6.86632	44.71	0.03382	0.01146
	MgCl ₂	0.10784	4.05986	15.1	7.23756	43.46	0.03399	0.01117
q = +56	KCl	0.11217	3.92972	18.36015	8.44096	43.80	0.03556	0.00914
	NaCl	0.10896	3.8354	17.855	8.11723	43.94	0.03657	0.00953
	CaCl ₂	0.10863	3.9424	18.29714	8.47359	43.60	0.03519	0.0092
	MgCl ₂	0.11672	4.03992	19.01531	8.52197	44.46	0.0355	0.00885
q = +84	KCl	0.10504	4.03736	29.75869	15.24394	39.34	0.02909	0.00563
	NaCl	0.08581	4.03548	31.19988	15.76293	39.64	0.0297	0.00536
	CaCl ₂	0.10229	3.92536	28.07036	14.0723	39.79	0.03049	0.00609
	MgCl ₂	0.10577	4.04257	28.04591	14.27144	39.58	0.02942	0.006

Table S.12. Same as Table S.10, but for the case of DND–COOH.

DND's Charge	Dissolved Salt	$\tau_{in}^{oh} / \text{ps}$	τ_c^{oh} / ps	τ_m^{oh} / ps	$\tau_{corr}^{oh} / \text{ps}$	$\theta_{tot}^{oh} / ^\circ$	$d_c^{oh} / \text{ps}^{-1}$	$d_m^{oh} / \text{ps}^{-1}$
q = 0	KCl	0.10894	3.25256	12.64887	4.48624	51.89	0.05509	0.01333
	NaCl	0.11073	3.29675	12.25895	4.23531	53.01	0.05599	0.01367
	CaCl ₂	0.11541	3.4871	12.46019	4.31982	53.14	0.05305	0.01346
	MgCl ₂	0.1136	3.41655	12.49947	4.30965	53.10	0.05412	0.01344
q = -28	KCl	0.11545	3.50032	20.04581	7.401	48.86	0.04706	0.00833
	NaCl	0.1148	3.45982	16.96733	6.17414	49.88	0.04907	0.00986
	CaCl ₂	0.11005	3.40945	18.14813	6.67398	49.28	0.04897	0.00922
	MgCl ₂	0.10978	3.47664	26.68515	10.69415	45.83	0.04319	0.00626
q = -56	KCl	0.11415	3.99713	32.73922	14.16831	43.57	0.03482	0.00516
	NaCl	0.11057	3.64795	25.13019	10.57239	44.77	0.03972	0.0067
	CaCl ₂	0.10822	3.62789	29.98238	12.91461	43.71	0.03842	0.00563
	MgCl ₂	0.0982	3.67278	43.12943	22.6804	37.76	0.02989	0.00391
q = -84	KCl	0.07335	3.42389	47.1118	26.72868	35.36	0.02863	0.00355
	NaCl	0.10961	3.65285	37.01562	17.04516	41.62	0.03531	0.00457
	CaCl ₂	0.09511	3.49052	42.96813	22.48444	37.86	0.03156	0.00393
	MgCl ₂	0.0733	3.54145	58.97455	35.07482	33.49	0.02531	0.0029

Table S.13. Same as Table S.10, but for the case of DND–OH.

DND's Charge	Dissolved Salt	$\tau_{in}^{oh} / \text{ps}$	τ_c^{oh} / ps	τ_m^{oh} / ps	$\tau_{corr}^{oh} / \text{ps}$	$\theta_{tot}^{oh} / ^\circ$	$d_c^{oh} / \text{ps}^{-1}$	$d_m^{oh} / \text{ps}^{-1}$
q = 0	KCl	0.11006	4.38607	11.18679	5.18982	46.84	0.03525	0.01498
	NaCl	0.08085	3.87792	10.22838	5.15341	43.81	0.03625	0.01633
	CaCl ₂	0.10231	4.16797	11.11882	5.26219	45.86	0.03599	0.0151
	MgCl ₂	0.09713	3.79553	9.92295	4.97572	43.94	0.03697	0.0169

S.2.2. Second hydration layer of DNDs

S.2.2.1. Water's dipole reorientation parameters

Table S.14. The EWIC parameters for the dipole reorientations of water in the second hydration layer of DND–H with various surface chemistries.

DND's Charge	Dissolved Salt	$\tau_{in}^{dip} / \text{ps}$	τ_c^{dip} / ps	τ_m^{dip} / ps	$\tau_{corr}^{dip} / \text{ps}$	$\theta_{tot}^{dip} / ^\circ$	$d_c^{dip} / \text{ps}^{-1}$	$d_m^{dip} / \text{ps}^{-1}$
q = 0	KCl	0.11166	2.69776	55.91193	4.53673	70.83	0.09131	0.00303
	NaCl	0.11181	2.69807	70.18191	5.05595	71.12	0.09152	0.00258
	CaCl ₂	0.11766	2.70751	185.57519	10.16271	71.40	0.09144	0.00099
	MgCl ₂	0.11428	2.77626	55.82115	5.21227	68.91	0.08724	0.00318
q = +28	KCl	0.11659	3.03506	38.75697	4.49298	67.95	0.07898	0.0046
	NaCl	0.11625	3.06894	31.97003	4.25949	66.97	0.07724	0.00551
	CaCl ₂	0.11491	3.04128	42.56867	4.73459	66.89	0.0778	0.00555
	MgCl ₂	0.12195	3.0783	56.03799	5.37553	68.08	0.07789	0.00395
q = +56	KCl	0.11639	3.2741	21.53006	4.14283	63.35	0.06904	0.00793
	NaCl	0.11668	3.29336	21.38162	4.13761	63.06	0.06832	0.0082
	CaCl ₂	0.09577	3.19266	24.5558	4.2908	63.99	0.07139	0.00714
	MgCl ₂	0.11576	3.31228	21.50806	4.11936	63.61	0.06852	0.00793
q = +84	KCl	0.09333	3.47179	19.09064	4.67155	59.27	0.06084	0.00893
	NaCl	0.11789	3.52715	19.97241	4.6794	59.54	0.06003	0.00892
	CaCl ₂	0.11972	3.48526	22.06182	4.53486	62.13	0.06367	0.00775
	MgCl ₂	0.09026	3.4093	18.21596	4.29187	60.11	0.06281	0.00965

Table S.15. Same as Table S.14, but for the case of DND–NH₂.

DND's Charge	Dissolved Salt	$\tau_{in}^{dip} / \text{ps}$	τ_c^{dip} / ps	τ_m^{dip} / ps	$\tau_{corr}^{dip} / \text{ps}$	$\theta_{tot}^{dip} / ^\circ$	$d_c^{dip} / \text{ps}^{-1}$	$d_m^{dip} / \text{ps}^{-1}$
q = 0	KCl	0.11553	3.24452	22.7759	3.65373	66.82	0.07299	0.00756
	NaCl	0.09292	3.1725	25.81392	3.84306	66.89	0.07462	0.00685
	CaCl ₂	0.11499	3.2577	23.73944	3.98874	65.32	0.07131	0.00733
	MgCl ₂	0.11997	3.31055	26.34426	4.05523	65.92	0.07065	0.00708
q = +28	KCl	0.1168	3.37811	19.28684	4.18067	61.58	0.06503	0.00908
	NaCl	0.11896	3.3954	20.15383	4.27448	61.46	0.06447	0.0089
	CaCl ₂	0.11027	3.27678	17.61771	4.02729	60.87	0.0662	0.00985
	MgCl ₂	0.11261	3.36678	17.7135	4.0532	61.15	0.06479	0.0097
q = +56	KCl	0.11666	3.49294	20.21763	5.1975	57.75	0.05872	0.0083
	NaCl	0.1117	3.3706	19.71152	5.13757	57.20	0.06015	0.00871
	CaCl ₂	0.11369	3.42455	17.00113	4.72925	56.95	0.05895	0.00988
	MgCl ₂	0.11491	3.42383	21.13236	5.06547	58.99	0.06139	0.00798
q = +84	KCl	0.1152	3.55162	22.5721	7.27609	51.78	0.05032	0.00744
	NaCl	0.11335	3.54414	20.72253	6.77191	51.89	0.0506	0.00807
	CaCl ₂	0.11756	3.59272	21.17412	6.65114	52.66	0.05085	0.00795

	MgCl ₂	0.11527	3.57153	20.57189	6.37947	53.20	0.05188	0.00816
--	-------------------	---------	---------	----------	---------	-------	---------	---------

Table S.16. Same as Table S.14, but for the case of DND–COOH.

DND's Charge	Dissolved Salt	$\tau_{in}^{dip} / \text{ps}$	τ_c^{dip} / ps	τ_m^{dip} / ps	$\tau_{corr}^{dip} / \text{ps}$	$\theta_{tot}^{dip} / ^\circ$	$d_c^{dip} / \text{ps}^{-1}$	$d_m^{dip} / \text{ps}^{-1}$
q = 0	KCl	0.09194	3.26783	16.81392	3.42549	64.44	0.07019	0.01029
	NaCl	0.11381	3.2675	16.67022	3.31789	65.48	0.07133	0.01006
	CaCl ₂	0.11976	3.36206	20.09611	3.62296	65.80	0.06951	0.00861
	MgCl ₂	0.11407	3.35238	16.75072	3.42015	64.24	0.06826	0.0108
q = -28	KCl	0.09455	3.27842	14.13868	3.33623	62.29	0.06768	0.0124
	NaCl	0.11442	3.30771	15.18724	3.50863	62.53	0.06748	0.01111
	CaCl ₂	0.11258	3.26397	22.42847	4.71541	60.85	0.06646	0.00771
	MgCl ₂	0.1201	3.42888	35.70922	7.94023	57.62	0.05967	0.00478
q = -56	KCl	0.11517	3.3366	13.3467	3.55792	60.10	0.06435	0.01253
	NaCl	0.06963	3.09128	16.31849	3.91419	59.69	0.0687	0.01081
	CaCl ₂	0.11379	3.3617	23.32952	6.39689	55.08	0.05763	0.00733
	MgCl ₂	0.09227	3.35022	35.28489	10.33152	51.85	0.05341	0.005
q = -84	KCl	0.11405	3.38643	13.90751	3.8241	56.73	0.06197	0.01205
	NaCl	0.11498	3.31587	15.98029	3.86546	57.42	0.0649	0.01087
	CaCl ₂	0.11545	3.41586	32.02352	9.14168	49.07	0.05383	0.00528
	MgCl ₂	0.11709	3.58314	45.13216	13.72688	48.33	0.04846	0.00386

Table S.17. Same as Table S.14, but for the case of DND–OH.

DND's Charge	Dissolved Salt	$\tau_{in}^{dip} / \text{ps}$	τ_c^{dip} / ps	τ_m^{dip} / ps	$\tau_{corr}^{dip} / \text{ps}$	$\theta_{tot}^{dip} / ^\circ$	$d_c^{dip} / \text{ps}^{-1}$	$d_m^{dip} / \text{ps}^{-1}$
q = 0	KCl	0.11619	3.14839	25.16275	3.55633	68.42	0.07651	0.00686
	NaCl	0.11282	3.21427	19.62693	3.39522	66.77	0.07355	0.00868
	CaCl ₂	0.11214	3.22398	25.15029	3.98545	65.97	0.0727	0.00706
	MgCl ₂	0.09594	3.15611	34.31474	4.42988	65.84	0.07384	0.00688

S.2.2.2. Water's OH reorientation parameters

Table S.18. The EWIC parameters for the OH reorientations of water in the second hydration layer of DND–H with various surface chemistries.

DND's Charge	Dissolved Salt	$\tau_{in}^{oh} / \text{ps}$	τ_c^{oh} / ps	τ_m^{oh} / ps	$\tau_{corr}^{oh} / \text{ps}$	$\theta_{tot}^{oh} / ^\circ$	$d_c^{oh} / \text{ps}^{-1}$	$d_m^{oh} / \text{ps}^{-1}$
q = 0	KCl	0.12169	2.54351	136.15496	6.88057	72.79	0.09827	0.00126
	NaCl	0.11899	2.46407	70.15369	4.8824	71.49	0.10069	0.00245
	CaCl ₂	0.11833	2.52006	74.73188	5.31104	71.08	0.09795	0.00223
	MgCl ₂	0.12603	2.60936	163.37722	9.0606	71.54	0.09495	0.00108
q = +28	KCl	0.12604	2.78015	52.00507	4.50472	70.60	0.08846	0.00323
	NaCl	0.12184	2.76796	59.58466	4.93594	70.20	0.08852	0.00306
	CaCl ₂	0.12801	2.80236	69.25819	5.11338	71.09	0.08811	0.0027

	MgCl₂	0.12728	2.80126	65.20207	5.27144	69.96	0.08726	0.00313
q = +56	KCl	0.12615	3.0623	28.78902	3.94791	67.62	0.07796	0.00605
	NaCl	0.12518	3.07253	26.95326	3.80498	66.91	0.07715	0.00719
	CaCl₂	0.1294	2.99448	32.39585	4.1205	67.75	0.07984	0.0056
	MgCl₂	0.12318	3.03606	31.9619	4.07838	68.04	0.07907	0.00548
q = +84	KCl	0.12529	3.49355	20.27677	4.09844	63.95	0.06533	0.00829
	NaCl	0.11995	3.50863	16.84356	3.92253	61.96	0.06305	0.01032
	CaCl₂	0.12525	3.45744	19.46282	3.85753	64.76	0.06671	0.00862
	MgCl₂	0.12303	3.39793	23.4116	4.08345	65.29	0.06832	0.00759

Table S.19. Same as Table S.18, but for the case of DND–NH₂.

DND's Charge	Dissolved Salt	$\tau_{in}^{oh} / \text{ps}$	τ_c^{oh} / ps	τ_m^{oh} / ps	$\tau_{corr}^{oh} / \text{ps}$	$\theta_{tot}^{oh} / ^\circ$	$d_c^{oh} / \text{ps}^{-1}$	$d_m^{oh} / \text{ps}^{-1}$
q = 0	KCl	0.1256	2.97739	44.97235	4.15747	70.60	0.0826	0.00435
	NaCl	0.1252	2.95322	67.93402	4.97107	71.23	0.08373	0.00324
	CaCl₂	0.12397	3.03407	36.78822	3.93837	69.81	0.0805	0.0051
	MgCl₂	0.12396	2.99647	53.49448	4.63889	70.29	0.08187	0.00383
q = +28	KCl	0.12611	3.29119	23.74634	3.68855	67.35	0.07233	0.00757
	NaCl	0.12374	3.27334	20.44107	3.58883	66.44	0.07199	0.0084
	CaCl₂	0.12244	3.23722	22.52328	3.705	66.08	0.07248	0.00842
	MgCl₂	0.12343	3.31093	20.00539	3.61084	66.40	0.07117	0.00836
q = +56	KCl	0.11609	3.53709	13.93016	3.84488	59.77	0.06023	0.01206
	NaCl	0.12102	3.53613	15.38809	3.78538	61.86	0.06246	0.01098
	CaCl₂	0.12183	3.42606	16.45334	3.71484	61.32	0.06343	0.01188
	MgCl₂	0.11913	3.45071	16.54705	3.76459	62.71	0.06475	0.01046
q = +84	KCl	0.11869	3.79764	13.93567	4.68234	54.27	0.04995	0.01228
	NaCl	0.12002	3.74762	13.26919	4.6145	53.84	0.05024	0.01274
	CaCl₂	0.11984	3.86104	13.379	4.41672	55.68	0.05086	0.01248
	MgCl₂	0.11141	3.74014	12.68319	4.25642	55.43	0.05218	0.01321

Table S.20. Same as Table S.18, but for the case of DND–COOH.

DND's Charge	Dissolved Salt	$\tau_{in}^{oh} / \text{ps}$	τ_c^{oh} / ps	τ_m^{oh} / ps	$\tau_{corr}^{oh} / \text{ps}$	$\theta_{tot}^{oh} / ^\circ$	$d_c^{oh} / \text{ps}^{-1}$	$d_m^{oh} / \text{ps}^{-1}$
q = 0	KCl	0.12117	3.17328	21.37023	3.35495	68.41	0.07589	0.00805
	NaCl	0.11983	3.13419	21.62062	3.26128	69.18	0.07754	0.00788
	CaCl₂	0.12445	3.18099	28.15779	3.55743	69.39	0.07645	0.00688
	MgCl₂	0.12113	3.27945	19.81092	3.29788	68.10	0.07326	0.00896
q = -28	KCl	0.12233	3.17748	20.51327	3.26178	68.66	0.07604	0.00838
	NaCl	0.12157	3.16474	19.43331	3.27376	67.85	0.07567	0.00877
	CaCl₂	0.11847	3.30643	18.31617	3.58878	64.84	0.06977	0.00963
	MgCl₂	0.12685	3.60622	17.4081	4.22293	61.27	0.06071	0.00959
q = -56	KCl	0.1209	3.29344	13.10035	3.08562	64.55	0.06982	0.01279
	NaCl	0.12228	3.17842	17.60842	3.29891	66.25	0.07397	0.00977

	CaCl ₂	0.12148	3.5258	15.03365	3.85385	61.08	0.06189	0.01109
	MgCl ₂	0.1197	3.65213	14.48403	4.7125	54.96	0.05291	0.01159
q = -84	KCl	0.12031	3.46558	11.82026	3.2452	61.78	0.06364	0.01417
	NaCl	0.09493	3.19332	13.13413	3.13321	63.32	0.07058	0.01312
	CaCl ₂	0.12045	3.60725	15.54391	4.50789	57.23	0.05625	0.0109
	MgCl ₂	0.11406	3.6089	16.1861	5.59508	52.25	0.0501	0.01049

Table S.21. Same as Table S.18, but for the case of DND–OH.

DND's Charge	Dissolved Salt	$\tau_{in}^{oh} / \text{ps}$	τ_c^{oh} / ps	τ_m^{oh} / ps	$\tau_{corr}^{oh} / \text{ps}$	$\theta_{tot}^{oh} / ^\circ$	$d_c^{oh} / \text{ps}^{-1}$	$d_m^{oh} / \text{ps}^{-1}$
q = 0	KCl	0.12246	2.94594	37.54282	3.71859	71.10	0.08379	0.00475
	NaCl	0.12487	2.97815	38.57316	3.73137	71.28	0.08306	0.00478
	CaCl ₂	0.12189	3.07883	23.98606	3.49739	68.39	0.07817	0.00727
	MgCl ₂	0.12571	3.01141	54.38633	4.53826	70.19	0.08131	0.00455

S.2.3. First hydration shell of ions (dissolved in aqueous solutions of the neutral DND–H)

S.2.3.1. Water's dipole reorientation parameters

Table S.22. The EWIC parameters for the dipole reorientations of water in the first hydration shell of different ions that are dissolved in the aqueous solution of the neutral DND–H.

Dissolved Ion	$\tau_{in}^{dip} / \text{ps}$	τ_c^{dip} / ps	τ_m^{dip} / ps	$\tau_{corr}^{dip} / \text{ps}$	$\theta_{tot}^{dip} / ^\circ$	$d_c^{dip} / \text{ps}^{-1}$	$d_m^{dip} / \text{ps}^{-1}$
K ⁺	0.0829	2.3039	7.42977	3.49639	44.71	0.06301	0.02249
Na ⁺	0.09689	2.05955	13.18624	6.49247	40.60	0.06011	0.01264
Ca ²⁺	0.05882	1.18104	20.78416	16.82372	21.55	0.03372	0.00802
Mg ²⁺	0.07922	1.43321	39.42366	34.28938	17.47	0.01858	0.00423
Cl ⁻ (KCl)	0.10111	4.30518	6.46691	3.31861	47.73	0.03701	0.02583
Cl ⁻ (NaCl)	0.1012	4.13089	6.52057	3.35873	46.67	0.037	0.02595
Cl ⁻ (CaCl ₂)	0.08199	4.05019	7.43666	3.48517	49.18	0.04087	0.02307
Cl ⁻ (MgCl ₂)	0.08274	4.11281	8.06629	3.66594	50.41	0.04193	0.02069

S.2.3.2. Water's OH reorientation parameters

Table S.23. Same as Table S.22, but for the case of OH reorientations.

Dissolved Ion	$\tau_{in}^{oh} / \text{ps}$	τ_c^{oh} / ps	τ_m^{oh} / ps	$\tau_{corr}^{oh} / \text{ps}$	$\theta_{tot}^{oh} / ^\circ$	$d_c^{oh} / \text{ps}^{-1}$	$d_m^{oh} / \text{ps}^{-1}$
K ⁺	0.08561	2.6476	4.37994	2.30627	45.67	0.05758	0.03858
Na ⁺	0.11331	2.9056	6.71265	2.74688	52.27	0.06225	0.02491
Ca ²⁺	0.08728	4.02615	10.40717	4.61461	49.23	0.04135	0.01611
Mg ²⁺	0.09371	5.94729	13.9436	8.73747	36.79	0.01763	0.01198
Cl ⁻ (KCl)	0.07496	2.19878	5.25782	3.9301	27.26	0.03213	0.03186
Cl ⁻ (NaCl)	0.06072	2.42466	5.33355	3.95745	27.98	0.03627	0.03151

Cl ⁻ (CaCl ₂)	0.07567	2.74527	5.1646	3.87307	27.65	0.02497	0.03234
Cl ⁻ (MgCl ₂)	0.06571	3.102	5.49449	3.97053	29.89	0.02774	0.03066

S.2.4. First hydration shell of Cations (dissolved in aqueous solutions of different DNDs)

The results of this sub-section differ from those of Section B.2.3 in the sense that the EWIC parameters here are presented for water in the first hydration shell of cations dissolved in the aqueous solutions of various DNDs with a distinct surface chemistry. As a reminder, only one DND particle is solvated in the solution.

S.2.4.1. Water's dipole reorientation parameters

Table S.24. The EWIC parameters for the dipole reorientations of water in the first hydration shell of different cations that are dissolved in the aqueous solutions of DND-H with various surface chemistries.

DND's Charge	Dissolved Cation	τ_{in}^{dip} / ps	τ_c^{dip} / ps	τ_m^{dip} / ps	τ_{corr}^{dip} / ps	θ_{tot}^{dip} / °	d_c^{dip} / ps ⁻¹	d_m^{dip} / ps ⁻¹
q = 0	K ⁺	0.0829	2.3039	7.42977	3.49639	44.71	0.06301	0.02249
	Na ⁺	0.09689	2.05955	13.18624	6.49247	40.60	0.06011	0.01264
	Ca ²⁺	0.05882	1.18104	20.78416	16.82372	21.55	0.03372	0.00802
	Mg ²⁺	0.07922	1.43321	39.42366	34.28938	17.47	0.01858	0.00423
q = +28	K ⁺	0.10374	2.40738	7.29096	3.47959	44.52	0.05954	0.02289
	Na ⁺	0.07619	1.9397	12.63357	6.37409	39.87	0.06209	0.0132
	Ca ²⁺	0.04724	1.12702	20.68639	16.73477	21.57	0.03631	0.00806
	Mg ²⁺	0.07979	1.56517	39.20475	34.01707	17.62	0.01796	0.00426
q = +56	K ⁺	0.10508	2.47426	7.88289	3.5578	45.92	0.06082	0.02138
	Na ⁺	0.09899	2.08028	12.92148	6.38736	40.54	0.05942	0.0129
	Ca ²⁺	0.04551	1.01164	20.55899	16.69122	21.38	0.03877	0.00811
	Mg ²⁺	0.08164	1.67836	40.72044	35.27044	17.73	0.01725	0.0041
q = +84	K ⁺	0.10437	2.47504	7.49595	3.5	45.27	0.05964	0.02226
	Na ⁺	0.09817	2.07532	12.9712	6.38938	40.60	0.05979	0.01288
	Ca ²⁺	0.04778	1.14513	21.07545	17.0369	21.61	0.03647	0.00791
	Mg ²⁺	0.0766	1.3072	39.46178	34.33365	17.45	0.02031	0.00422

Table S.25. Same as Table S.24, but for the case of DND-NH₂.

DND's Charge	Dissolved Cation	τ_{in}^{dip} / ps	τ_c^{dip} / ps	τ_m^{dip} / ps	τ_{corr}^{dip} / ps	θ_{tot}^{dip} / °	d_c^{dip} / ps ⁻¹	d_m^{dip} / ps ⁻¹
q = 0	K ⁺	0.10781	2.56877	8.28298	3.70633	46.25	0.05917	0.02018
	Na ⁺	0.10087	2.19523	14.03397	6.81992	40.95	0.05721	0.01189
	Ca ²⁺	0.05709	1.09998	20.86294	16.88738	21.53	0.03592	0.00799
	Mg ²⁺	0.08061	1.69753	41.65024	36.04191	17.78	0.01692	0.00401
q = +28	K ⁺	0.1018	2.38184	7.52371	3.50642	45.12	0.06159	0.02219
	Na ⁺	0.07964	2.01229	12.91599	6.39736	40.42	0.06151	0.01292
	Ca ²⁺	0.05788	1.15195	20.79339	16.83256	21.54	0.03507	0.00802
	Mg ²⁺	0.07846	1.4283	40.27604	34.96305	17.59	0.019	0.00414
q = +56	K ⁺	0.08983	2.54325	7.88044	3.53479	46.38	0.0605	0.0213

	Na ⁺	0.09815	2.11124	13.1076	6.44505	40.69	0.0589	0.01273
	Ca ²⁺	0.04523	0.97869	20.43708	16.59763	21.35	0.04109	0.00816
	Mg ²⁺	0.08057	1.53559	39.44362	34.26602	17.55	0.01771	0.00423
q = +84	K ⁺	0.1046	2.4729	7.5373	3.48915	45.50	0.05999	0.02216
	Na ⁺	0.09965	2.11818	13.38417	6.51263	40.95	0.05956	0.01246
	Ca ²⁺	0.05576	1.06158	20.66181	16.75036	21.45	0.03729	0.00807
	Mg ²⁺	0.07908	1.43758	39.74972	34.54095	17.53	0.01918	0.0042

Table S.26. Same as Table S.24, but for the case of DND–COOH.

DND's Charge	Dissolved Cation	$\tau_{in}^{dip} / \text{ps}$	τ_c^{dip} / ps	τ_m^{dip} / ps	$\tau_{corr}^{dip} / \text{ps}$	$\theta_{tot}^{dip} / ^\circ$	$d_c^{dip} / \text{ps}^{-1}$	$d_m^{dip} / \text{ps}^{-1}$
q = 0	K ⁺	0.12026	2.81633	11.28367	4.18538	50.42	0.06114	0.01504
	Na ⁺	0.09876	2.13954	13.72261	6.70414	40.81	0.0584	0.01215
	Ca ²⁺	0.05595	1.10087	21.20264	17.16102	21.54	0.03683	0.00786
	Mg ²⁺	0.0797	1.62684	40.51071	35.07157	17.77	0.01764	0.00412
q = -28	K ⁺	0.12337	2.86127	17.12025	5.67332	51.28	0.06166	0.00982
	Na ⁺	0.10431	2.33108	15.90806	7.52812	41.52	0.05515	0.0105
	Ca ²⁺	0.0644	1.59551	23.89434	19.05123	22.33	0.02663	0.00698
	Mg ²⁺	0.08111	1.81068	45.13935	39.07959	17.75	0.01535	0.0037
q = -56	K ⁺	0.10259	2.88231	26.00231	8.04311	51.28	0.06136	0.00646
	Na ⁺	0.10479	2.39186	17.01082	8.01448	41.57	0.05377	0.0098
	Ca ²⁺	0.07342	2.40611	27.62062	21.53628	23.49	0.01939	0.00604
	Mg ²⁺	0.08171	2.18812	51.71268	44.50497	18.13	0.01329	0.00323
q = -84	K ⁺	0.12602	2.93766	33.94203	10.61855	50.36	0.05854	0.00493
	Na ⁺	0.08752	2.5616	22.12357	10.14302	41.90	0.05122	0.00757
	Ca ²⁺	0.07173	2.39859	31.56679	24.64478	23.39	0.01951	0.00528
	Mg ²⁺	0.08208	2.47971	56.26651	48.3798	18.18	0.01239	0.00297

Table S.27. Same as Table S.24, but for the case of DND–OH.

DND's Charge	Dissolved Cation	$\tau_{in}^{dip} / \text{ps}$	τ_c^{dip} / ps	τ_m^{dip} / ps	$\tau_{corr}^{dip} / \text{ps}$	$\theta_{tot}^{dip} / ^\circ$	$d_c^{dip} / \text{ps}^{-1}$	$d_m^{dip} / \text{ps}^{-1}$
q = 0	K ⁺	0.10823	2.57418	8.55948	3.71305	47.08	0.06062	0.01952
	Na ⁺	0.09595	2.08316	13.50571	6.63965	40.61	0.05954	0.01235
	Ca ²⁺	0.03429	0.94298	20.90945	16.96591	21.39	0.04212	0.00797
	Mg ²⁺	0.08414	1.87546	40.99642	35.48122	17.80	0.01478	0.00407

S.2.4.2. Water's OH reorientation parameters

Table S.28. The EWIC parameters for the OH reorientations of water in the first hydration shell of different cations that are dissolved in the aqueous solutions of DND–H with various surface chemistries.

DND's Charge	Dissolved Cation	$\tau_{in}^{oh} / \text{ps}$	τ_c^{oh} / ps	τ_m^{oh} / ps	$\tau_{corr}^{oh} / \text{ps}$	$\theta_{tot}^{oh} / ^\circ$	$d_c^{oh} / \text{ps}^{-1}$	$d_m^{oh} / \text{ps}^{-1}$
q = 0	K ⁺	0.08561	2.6476	4.37994	2.30627	45.67	0.05758	0.03858
	Na ⁺	0.11331	2.9056	6.71265	2.74688	52.27	0.06225	0.02491

	Ca ²⁺	0.08728	4.02615	10.40717	4.61461	49.23	0.04135	0.01611
	Mg ²⁺	0.09371	5.94729	13.9436	8.73747	36.79	0.01763	0.01198
q = +28	K ⁺	0.10831	3.0176	4.49228	2.31145	47.88	0.05307	0.03718
	Na ⁺	0.11209	2.92592	6.43637	2.73114	51.43	0.0605	0.02595
	Ca ²⁺	0.10774	4.07014	10.09485	4.60654	48.53	0.04005	0.01656
	Mg ²⁺	0.09186	5.36433	12.96585	8.4724	34.71	0.01773	0.01289
	K ⁺	0.10652	2.99128	4.61418	2.3244	48.59	0.05479	0.03616
q = +56	Na ⁺	0.11231	2.91551	6.46461	2.70885	51.85	0.0614	0.02584
	Ca ²⁺	0.08671	3.97347	10.11479	4.63034	48.23	0.04074	0.01654
	Mg ²⁺	0.07034	5.64109	13.89368	8.73885	36.36	0.01826	0.01204
	K ⁺	0.10971	3.12665	4.86287	2.33356	50.70	0.05553	0.03437
q = +84	Na ⁺	0.1123	2.93538	6.75996	2.72377	52.94	0.06273	0.02471
	Ca ²⁺	0.1119	4.234	10.61605	4.65831	49.82	0.03999	0.01576
	Mg ²⁺	0.11455	5.85812	13.6981	8.68274	36.20	0.01743	0.01222
	K ⁺	0.10971	3.12665	4.86287	2.33356	50.70	0.05553	0.03437

Table S.29. Same as Table S.28, but for the case of DND–NH₂.

DND's Charge	Dissolved Cation	τ_{in}^{oh} / ps	τ_c^{oh} / ps	τ_m^{oh} / ps	τ_{corr}^{oh} / ps	θ_{tot}^{oh} / °	d_c^{oh} / ps ⁻¹	d_m^{oh} / ps ⁻¹
q = 0	K ⁺	0.11064	2.99682	5.37772	2.43437	51.22	0.05838	0.03152
	Na ⁺	0.11594	3.02245	7.41656	2.85511	53.93	0.06242	0.02249
	Ca ²⁺	0.10749	4.06692	10.56723	4.66731	49.34	0.04106	0.0158
	Mg ²⁺	0.11348	5.6313	13.71199	8.79784	35.48	0.01757	0.0122
q = +28	K ⁺	0.11071	3.11902	4.92157	2.30477	51.24	0.05598	0.03457
	Na ⁺	0.11467	2.96315	6.80025	2.73977	52.95	0.06213	0.02457
	Ca ²⁺	0.09093	4.06027	10.60568	4.6282	49.44	0.04116	0.016
	Mg ²⁺	0.09442	5.65596	13.29246	8.60366	35.32	0.01736	0.01255
q = +56	K ⁺	0.10461	2.8119	4.52582	2.31847	47.31	0.05585	0.03703
	Na ⁺	0.1151	3.00857	6.83476	2.74446	53.19	0.06154	0.02445
	Ca ²⁺	0.10774	4.05987	10.10527	4.60275	48.61	0.04026	0.01651
	Mg ²⁺	0.11649	5.67856	13.08744	8.53452	35.05	0.01701	0.01274
q = +84	K ⁺	0.10306	2.76817	4.39148	2.29673	46.21	0.05448	0.03848
	Na ⁺	0.09009	2.71314	6.54478	2.73721	51.10	0.06484	0.02566
	Ca ²⁺	0.08921	4.01065	10.52938	4.64781	49.19	0.04141	0.01596
	Mg ²⁺	0.1154	6.06067	13.98069	8.67218	37.19	0.01763	0.01199

Table S.30. Same as Table S.28, but for the case of DND–COOH.

DND's Charge	Dissolved Cation	τ_{in}^{oh} / ps	τ_c^{oh} / ps	τ_m^{oh} / ps	τ_{corr}^{oh} / ps	θ_{tot}^{oh} / °	d_c^{oh} / ps ⁻¹	d_m^{oh} / ps ⁻¹
q = 0	K ⁺	0.11516	2.95992	6.49016	2.51658	54.76	0.06469	0.02652
	Na ⁺	0.11622	3.01206	7.18212	2.80619	53.60	0.06209	0.02327
	Ca ²⁺	0.10767	4.02656	10.33512	4.68678	48.47	0.04045	0.01617
	Mg ²⁺	0.1153	5.59997	13.81202	8.8038	35.73	0.01784	0.01209
q = -28	K ⁺	0.13503	2.95695	13.95883	3.39718	60.94	0.07353	0.0122

	Na ⁺	0.11568	2.87198	8.43444	3.12732	53.20	0.06446	0.01991
	Ca ²⁺	0.08666	3.88429	11.68916	5.09349	48.49	0.04196	0.01434
	Mg ²⁺	0.11597	5.98671	16.47864	9.93664	37.45	0.01805	0.01018
q = -56	K ⁺	0.13682	2.90394	19.73639	4.60185	58.98	0.07233	0.00856
	Na ⁺	0.12316	3.0124	10.2809	3.42259	55.20	0.06448	0.01628
	Ca ²⁺	0.11182	4.03976	13.75981	5.63476	49.49	0.04152	0.01219
	Mg ²⁺	0.11633	6.02653	18.37792	10.99922	37.41	0.01791	0.00908
q = -84	K ⁺	0.13628	2.8651	32.59284	7.22947	57.42	0.07115	0.00515
	Na ⁺	0.12395	3.05397	13.85178	4.30218	54.85	0.0631	0.01207
	Ca ²⁺	0.11001	4.05022	16.6068	6.68035	48.85	0.04065	0.01006
	Mg ²⁺	0.11463	6.07132	20.78753	12.17721	37.65	0.01798	0.00805

Table S.31. Same as Table S.28, but for the case of DND–OH.

DND's Charge	Dissolved Cation	τ_{in}^{oh} / ps	τ_c^{oh} / ps	τ_m^{oh} / ps	τ_{corr}^{oh} / ps	$\theta_{tot}^{oh} / ^\circ$	d_c^{oh} / ps^{-1}	d_m^{oh} / ps^{-1}
q = 0	K ⁺	0.11203	2.99982	5.07244	2.38171	50.10	0.05659	0.03353
	Na ⁺	0.11029	2.85722	6.59047	2.78359	51.18	0.06165	0.02533
	Ca ²⁺	0.1076	4.06457	10.39022	4.66934	48.87	0.04058	0.01606
	Mg ²⁺	0.12017	6.24464	14.70689	8.9684	37.83	0.01759	0.01139

S.2.5. First hydration shell of Cl⁻ anion (dissolved in aqueous solutions of different DNDs)

S.2.5.1. Water's dipole reorientation parameters

Table S.32. The EWIC parameters for the dipole reorientations of water in the first hydration shell of Cl⁻ anions of different salts that are dissolved in the aqueous solutions of DND–H with various surface chemistries.

DND's Charge	Dissolved Anion	τ_{in}^{dip} / ps	τ_c^{dip} / ps	τ_m^{dip} / ps	τ_{corr}^{dip} / ps	$\theta_{tot}^{dip} / ^\circ$	d_c^{dip} / ps^{-1}	d_m^{dip} / ps^{-1}
q = 0	Cl ⁻ (KCl)	0.10111	4.30518	6.46691	3.31861	47.73	0.03701	0.02583
	Cl ⁻ (NaCl)	0.1012	4.13089	6.52057	3.35873	46.67	0.037	0.02595
	Cl ⁻ (CaCl ₂)	0.08199	4.05019	7.43666	3.48517	49.18	0.04087	0.02307
	Cl ⁻ (MgCl ₂)	0.08274	4.11281	8.06629	3.66594	50.41	0.04193	0.02069
q = +28	Cl ⁻ (KCl)	0.06195	3.73992	6.29004	3.37229	44.63	0.03894	0.02676
	Cl ⁻ (NaCl)	0.10432	4.3642	7.35205	3.46001	50.00	0.03874	0.02308
	Cl ⁻ (CaCl ₂)	0.102	4.27495	7.45701	3.58841	49.01	0.0387	0.02242

	Cl ⁻ (MgCl ₂)	0.10733	3.99629	12.9181	4.32059	56.03	0.04948	0.01297
q = +56	Cl ⁻ (KCl)	0.10436	4.17102	9.18871	3.9197	51.48	0.04243	0.01825
	Cl ⁻ (NaCl)	0.10564	4.159	9.09119	3.94701	50.88	0.04193	0.0184
	Cl ⁻ (CaCl ₂)	0.10241	4.12893	9.07887	3.96554	50.69	0.04204	0.01837
	Cl ⁻ (MgCl ₂)	0.08546	3.91666	12.00458	4.49783	52.94	0.04703	0.01393
	Cl ⁻ (KCl)	0.10467	4.06102	11.20408	4.41476	52.23	0.04454	0.0149
q = +84	Cl ⁻ (NaCl)	0.10694	4.07264	11.71443	4.53969	52.25	0.04438	0.01432
	Cl ⁻ (CaCl ₂)	0.10687	4.17126	10.85512	4.23582	53.10	0.04431	0.01537
	Cl ⁻ (MgCl ₂)	0.10925	4.03769	13.90305	4.76069	54.51	0.04733	0.0121
	Cl ⁻ (MgCl ₂)	0.10925	4.03769	13.90305	4.76069	54.51	0.04733	0.0121

Table S.33. Same as Table S.32, but for the case of DND–NH₂.

DND's Charge	Dissolved Anion	$\tau_{in}^{dip} / \text{ps}$	τ_c^{dip} / ps	τ_m^{dip} / ps	$\tau_{corr}^{dip} / \text{ps}$	$\theta_{tot}^{dip} / ^\circ$	$d_c^{dip} / \text{ps}^{-1}$	$d_m^{dip} / \text{ps}^{-1}$
q = 0	Cl ⁻ (KCl)	0.10095	4.30464	6.47757	3.33038	47.61	0.03681	0.02582
	Cl ⁻ (NaCl)	0.10371	4.49074	7.14219	3.40639	50.48	0.03836	0.02346
	Cl ⁻ (CaCl ₂)	0.10075	4.33328	7.19086	3.48013	49.33	0.03848	0.02329
	Cl ⁻ (MgCl ₂)	0.10987	4.13048	12.25587	4.10686	56.58	0.04837	0.01391
q = +28	Cl ⁻ (KCl)	0.06435	3.80757	7.06922	3.51827	46.68	0.04049	0.02405
	Cl ⁻ (NaCl)	0.10195	4.17747	7.36069	3.54923	48.77	0.03924	0.02276
	Cl ⁻ (CaCl ₂)	0.10535	4.28422	8.67251	3.71062	52.14	0.04198	0.01945
	Cl ⁻ (MgCl ₂)	0.10532	4.11865	9.99276	3.9426	53.45	0.04525	0.01675
q = +56	Cl ⁻ (KCl)	0.10974	4.18946	12.73189	4.23439	56.85	0.04807	0.01317
	Cl ⁻ (NaCl)	0.1103	4.21056	12.56465	4.20909	56.21	0.04707	0.01378
	Cl ⁻ (CaCl ₂)	0.10616	4.1493	11.05887	4.10435	54.49	0.04601	0.01521
	Cl ⁻ (MgCl ₂)	0.10893	3.97426	15.84387	4.82973	56.79	0.05059	0.01054
q = +84	Cl ⁻	0.09093	3.74782	27.82691	7.00459	56.82	0.05368	0.00614

	(KCl)							
	Cl ⁻ (NaCl)	0.09095	3.74982	31.68966	7.73457	56.83	0.05367	0.00538
	Cl ⁻ (CaCl ₂)	0.11227	3.85677	23.57192	6.04767	57.69	0.05312	0.00712
	Cl ⁻ (MgCl ₂)	0.11359	3.79735	31.30362	7.36536	57.57	0.0538	0.0055

Table S.34. Same as Table S.32, but for the case of DND–COOH.

DND's Charge	Dissolved Anion	τ_{in}^{dip} / ps	τ_c^{dip} / ps	τ_m^{dip} / ps	τ_{corr}^{dip} / ps	θ_{tot}^{dip} / °	d_c^{dip} / ps ⁻¹	d_m^{dip} / ps ⁻¹
q = 0	Cl ⁻ (KCl)	0.10287	4.4629	7.34205	3.34511	52.22	0.04042	0.02288
	Cl ⁻ (NaCl)	0.10317	4.4915	6.79874	3.35595	49.47	0.03727	0.02462
	Cl ⁻ (CaCl ₂)	0.10426	4.45876	7.84523	3.53992	51.88	0.0402	0.02126
	Cl ⁻ (MgCl ₂)	0.10738	4.05563	12.66128	4.18742	56.72	0.04955	0.01331
q = -28	Cl ⁻ (KCl)	0.10427	4.32519	6.84537	3.33346	49.31	0.03812	0.02476
	Cl ⁻ (NaCl)	0.08157	4.10978	7.22297	3.41528	49.59	0.04071	0.02341
	Cl ⁻ (CaCl ₂)	0.07835	4.02917	7.33266	3.52546	48.27	0.03991	0.02322
	Cl ⁻ (MgCl ₂)	0.10591	4.09227	10.52254	3.97368	54.46	0.04666	0.01588
q = -56	Cl ⁻ (KCl)	0.10165	4.3766	6.95712	3.31491	49.93	0.0384	0.02461
	Cl ⁻ (NaCl)	0.10409	4.43739	7.43004	3.3662	51.66	0.03983	0.02303
	Cl ⁻ (CaCl ₂)	0.1003	4.15173	7.28211	3.53722	48.60	0.03936	0.02293
	Cl ⁻ (MgCl ₂)	0.10882	4.16289	11.54029	4.06613	56.06	0.04755	0.01446
q = -84	Cl ⁻ (KCl)	0.1017	4.40215	6.96218	3.33738	50.27	0.03897	0.02412
	Cl ⁻ (NaCl)	0.09927	4.15825	6.47393	3.36329	46.74	0.03708	0.02583
	Cl ⁻ (CaCl ₂)	0.10017	4.19963	7.59406	3.56701	49.72	0.04017	0.02205
	Cl ⁻ (MgCl ₂)	0.10552	3.97389	13.03641	4.32569	56.16	0.04992	0.01286

Table S.35. Same as Table S.32, but for the case of DND–OH.

DND's Charge	Dissolved Anion	τ_{in}^{dip} / ps	τ_c^{dip} / ps	τ_m^{dip} / ps	τ_{corr}^{dip} / ps	θ_{tot}^{dip} / °	d_c^{dip} / ps ⁻¹	d_m^{dip} / ps ⁻¹
--------------	-----------------	------------------------	---------------------	---------------------	--------------------------	--------------------------	--------------------------------	--------------------------------

q = 0	Cl⁻ (KCl)	0.10273	4.35392	6.85163	3.34214	49.60	0.0385	0.02448
	Cl⁻ (NaCl)	0.10215	4.33332	6.92401	3.36584	49.41	0.03844	0.02433
	Cl⁻ (CaCl₂)	0.10169	4.28269	7.74529	3.54251	50.57	0.04025	0.02183
	Cl⁻ (MgCl₂)	0.08681	4.10702	10.85455	3.93843	55.45	0.04752	0.01557

S.2.5.2. Water's OH reorientation parameters

Table S.36. The EWIC parameters for the OH reorientations of water in the first hydration shell of Cl⁻ anions of different salts that are dissolved in the aqueous solutions of DND-H with various surface chemistries.

DND's Charge	Dissolved Anion	τ_{in}^{oh} / ps	τ_c^{oh} / ps	τ_m^{oh} / ps	τ_{corr}^{oh} / ps	$\theta_{tot}^{oh} / ^\circ$	d_c^{oh} / ps^{-1}	d_m^{oh} / ps^{-1}
q = 0	Cl⁻ (KCl)	0.07496	2.19878	5.25782	3.9301	27.25958	0.03213	0.03186
	Cl⁻ (NaCl)	0.06072	2.42466	5.33355	3.95745	27.97642	0.03627	0.03151
	Cl⁻ (CaCl₂)	0.07567	2.74527	5.1646	3.87307	27.64849	0.02497	0.03234
	Cl⁻ (MgCl₂)	0.06571	3.102	5.49449	3.97053	29.88851	0.02774	0.03066
q = +28	Cl⁻ (KCl)	0.05929	1.8652	5.30959	4.00335	26.50711	0.03509	0.03149
	Cl⁻ (NaCl)	0.08124	2.82702	5.50849	4.0569	28.5682	0.02438	0.03029
	Cl⁻ (CaCl₂)	0.07408	2.51962	5.29185	3.95694	27.55377	0.02727	0.03159
	Cl⁻ (MgCl₂)	0.06963	4.47112	6.22991	4.14595	35.78006	0.0232	0.02691
q = +56	Cl⁻ (KCl)	0.07348	4.65896	7.40723	4.57301	38.84231	0.02468	0.02264
	Cl⁻ (NaCl)	0.0907	4.59397	7.10931	4.5421	37.28642	0.02348	0.02349
	Cl⁻ (CaCl₂)	0.06931	4.62422	6.6516	4.33672	36.69061	0.02263	0.02511
	Cl⁻ (MgCl₂)	0.07034	4.79916	7.34505	4.50463	39.44549	0.02457	0.02283
q = +84	Cl⁻ (KCl)	0.09219	4.86263	8.50258	5.0041	40.57234	0.02541	0.01966
	Cl⁻ (NaCl)	0.09135	4.72841	8.37236	4.99535	39.80806	0.02532	0.01999
	Cl⁻ (CaCl₂)	0.08892	5.2318	7.5464	4.55496	40.76633	0.0238	0.02213
	Cl⁻ (MgCl₂)	0.09239	5.47368	8.63565	4.72704	44.61895	0.02612	0.01951

Table S.37. Same as Table S.36, but for the case of DND–NH₂.

DND's Charge	Dissolved Anion	$\tau_{in}^{oh} / \text{ps}$	τ_c^{oh} / ps	τ_m^{oh} / ps	$\tau_{corr}^{oh} / \text{ps}$	$\theta_{tot}^{oh} / ^\circ$	$d_c^{oh} / \text{ps}^{-1}$	$d_m^{oh} / \text{ps}^{-1}$
q = 0	Cl ⁻ (KCl)	0.08089	3.01486	5.43968	3.97258	29.28	0.02407	0.03075
	Cl ⁻ (NaCl)	0.06551	2.56759	5.33065	3.98216	27.67	0.02659	0.03127
	Cl ⁻ (CaCl ₂)	0.06293	2.62912	5.17598	3.90302	27.25	0.0284	0.03223
	Cl ⁻ (MgCl ₂)	0.08721	4.96601	6.27592	4.1197	37.13	0.02175	0.02666
q = +28	Cl ⁻ (KCl)	0.08155	2.89874	5.75035	4.16029	29.51	0.02607	0.02909
	Cl ⁻ (NaCl)	0.06477	2.73257	5.65733	4.13556	28.86	0.02551	0.02948
	Cl ⁻ (CaCl ₂)	0.082	3.98649	5.74785	4.06664	32.00	0.02152	0.02904
	Cl ⁻ (MgCl ₂)	0.06839	4.10656	6.06432	4.1617	33.70	0.02228	0.0275
q = +56	Cl ⁻ (KCl)	0.07537	4.47183	7.35601	4.55179	38.42	0.02574	0.02283
	Cl ⁻ (NaCl)	0.09306	5.11155	7.69901	4.54368	41.25	0.02476	0.02196
	Cl ⁻ (CaCl ₂)	0.0871	5.21988	6.61923	4.23616	38.53	0.02177	0.02524
	Cl ⁻ (MgCl ₂)	0.09204	5.66075	7.71749	4.44123	43.80	0.02465	0.02162
q = +84	Cl ⁻ (KCl)	0.10006	5.0739	13.68711	5.86106	49.85	0.0334	0.01229
	Cl ⁻ (NaCl)	0.09757	4.98022	14.84992	6.10119	50.26	0.03437	0.01145
	Cl ⁻ (CaCl ₂)	0.07504	5.16016	10.24247	4.91232	48.20	0.03111	0.01659
	Cl ⁻ (MgCl ₂)	0.09363	5.19919	11.87598	5.23552	50.18	0.03281	0.01426

Table S.38. Same as Table S.36, but for the case of DND–COOH.

DND's Charge	Dissolved Anion	$\tau_{in}^{oh} / \text{ps}$	τ_c^{oh} / ps	τ_m^{oh} / ps	$\tau_{corr}^{oh} / \text{ps}$	$\theta_{tot}^{oh} / ^\circ$	$d_c^{oh} / \text{ps}^{-1}$	$d_m^{oh} / \text{ps}^{-1}$
q = 0	Cl ⁻ (KCl)	0.08017	3.17152	5.46387	3.9653	29.86	0.02437	0.03059
	Cl ⁻ (NaCl)	0.06838	3.11458	5.45194	3.98589	29.32	0.02458	0.03063
	Cl ⁻ (CaCl ₂)	0.07746	2.75905	5.19926	3.90777	27.47	0.02364	0.03208

	Cl ⁻ (MgCl ₂)	0.08575	4.7025	6.05898	4.0806	35.31	0.02091	0.02768
q = -28	Cl ⁻ (KCl)	0.08465	3.93567	5.57838	3.9706	31.85	0.02462	0.03006
	Cl ⁻ (NaCl)	0.08114	3.50291	5.68098	4.01304	31.68	0.02602	0.02951
	Cl ⁻ (CaCl ₂)	0.07164	2.1316	5.03584	3.87014	25.75	0.03167	0.03312
	Cl ⁻ (MgCl ₂)	0.08186	3.89672	5.9299	4.09012	33.27	0.02299	0.02822
	Cl ⁻ (KCl)	0.07893	3.11591	5.38601	3.95653	29.23	0.02696	0.03103
q = -56	Cl ⁻ (NaCl)	0.09174	5.08129	6.40576	3.98448	40.01	0.02332	0.02689
	Cl ⁻ (CaCl ₂)	0.07368	2.18292	5.10083	3.87894	26.33	0.02762	0.0327
	Cl ⁻ (MgCl ₂)	0.07009	4.24562	5.94324	4.08192	33.93	0.02235	0.02812
	Cl ⁻ (KCl)	0.08434	3.38336	5.45375	3.97924	29.69	0.02143	0.0306
q = -84	Cl ⁻ (NaCl)	0.07915	2.51967	5.36294	4.00315	27.62	0.02594	0.03112
	Cl ⁻ (CaCl ₂)	0.07777	2.93266	5.36266	3.95985	28.59	0.02331	0.03112
	Cl ⁻ (MgCl ₂)	0.08632	4.77948	6.22799	4.12085	36.34	0.02155	0.02692
	Cl ⁻ (KCl)	0.08434	3.38336	5.45375	3.97924	29.69	0.02143	0.0306

Table S.39. Same as Table S.36, but for the case of DND–OH.

DND's Charge	Dissolved Anion	τ_{in}^{oh} / ps	τ_c^{oh} / ps	τ_m^{oh} / ps	τ_{corr}^{oh} / ps	$\theta_{tot}^{oh} / ^\circ$	d_c^{oh} / ps^{-1}	d_m^{oh} / ps^{-1}
q = 0	Cl ⁻ (KCl)	0.07422	1.89694	5.09847	3.92837	25.41	0.03056	0.03271
	Cl ⁻ (NaCl)	0.06327	2.49872	5.32979	3.97883	27.66	0.03382	0.03141
	Cl ⁻ (CaCl ₂)	0.06349	3.11982	5.41132	3.92411	30.27	0.03001	0.03107
	Cl ⁻ (MgCl ₂)	0.08629	4.77373	6.04898	4.07268	35.59	0.02076	0.02767

References

1. Efron, B. & Tibshirani, R. An Introduction to the Bootstrap. (Chapman and Hall, 1993).